BBA - Gene Regulatory Mechanisms 1862 (2019) 194404

Contents lists available at ScienceDirect

BBA - Gene Regulatory Mechanisms

journal homepage: www.elsevier.com/locate/bbagrm

HOXA2 activity regulation by cytoplasmic relocation, protein stabilization and post-translational modification

Noémie Deneyer[a], Laure Bridoux[a], Céline Bombled[a], Tamara Pringels[a], Isabelle Bergiers[a], Sébastien Pyr dit Ruys[b], Didier Vertommen[b], Jean-Claude Twizere[c], René Rezsohazy[a,*]

[a] Animal Molecular and Cellular Biology group (AMCB), Louvain Institute of Biomolecular Science and Technology (LIBST), UCLouvain, Croix du sud 4-5, 1348 Louvain-la-Neuve, Belgium
[b] Faculty of Medicine, de Duve Institute, UCLouvain, Avenue Hippocrate 75 bte 74.02, 1200-Brussels, Belgium
[c] Laboratory of Viral Interactomes and Network Biology, GIGA Institute, University of Liège, 4000 Liège, Belgium

ARTICLE INFO

Keywords:
HOX
PPP1CB
KPC2
Activity regulation
Nucleocytoplasmic shuttling
Post-translational modifications

ABSTRACT

HOX proteins are homeodomain transcription factors critically involved in patterning animal embryos and controlling organogenesis. While the functions of HOX proteins and the processes under their control begin to be well documented, the modalities of HOX protein activity regulation remain poorly understood. Here we show that HOXA2 interacts with PPP1CB, a catalytic subunit of the Ser/Thr PP1 phosphatase complex. This interaction co-localizes in the cytoplasm with a previously described HOXA2 interactor, KPC2, which belongs to the KPC E3 ubiquitin ligase complex. We provide evidence that HOXA2, PPP1CB and KPC2 define a molecularly and functionally interacting complex. Collectively, our experiments support that PPP1CB and KPC2 together inhibit the activity of HOXA2 by activating its nuclear export, but favored HOXA2 de-ubiquitination and stabilization thereby establishing a store of HOXA2 in the cytoplasm.

1. Introduction

Since their discovery in *Drosophila* forty years ago, extensive studies have increased our knowledge about the roles and functions of the Homeobox (*HOX*) genes. *HOX* genes, which are often qualified as embryo architects, are well-known for coding transcription factors involved in animal development, and in particular in anteroposterior and appendicular axis patterning [1,2]. Given their essential patterning functions, *Hox* gene mutations lead to homeotic transformations. These transformations are characterized by the substitution of an embryonic structure by another one, ectopically positioned. In human, *HOX* mutations can also lead to malformations and diseases, although most are supposed to be lethal like in mouse knockout models [3].

In order to characterize HOX transcription factor activity in relationship with their embryonic functions, many studies have focused on the identification of their downstream target genes (reviewed in [4,5]). Investigation about HOX protein activity also identified TALE (three amino acid loop extension) homeodomain proteins, which are important cofactors contributing to the selective binding of HOX proteins on target loci [5–8].

In spite of important advances in the identification of downstream effectors of HOX proteins, and contrary to other well-studied transcription factors such as p53 [9] or NF-κB [10,11], very little is known about how the activity of HOX proteins may be modulated at the cellular level. One way to modulate protein activity is by the addition of post-translational modifications (PTMs). The few studies approaching this issue support that PTMs could drastically affect HOX protein stability and capacity to bind DNA or to modulate transcription (reviewed in [13,14]). Among the most documented cases, HOXA10 appears to be acetylated, SUMOylated as well as phosphorylated. These PTMs have been shown to affect both HOXA10 stability and activity [15–18]. Activity regulation of HOX proteins can also be mediated by their interaction with cofactors [5–8]. As an example, the *Drosophila* TALE protein Extradenticle (EXD) not only plays a role in increasing the DNA binding specificity of the HOX protein Deformed (DFD), but also acts in stimulating its transcriptional activation capacity [19]. The trans-activation domain of DFD is indeed inhibited by the DNA-binding homeodomain (HD), and the EXD-to-HD interaction is required to relieve this

Abbreviations: HOX, homeobox; HOXA2, Homeobox protein HOX-A2; KPC2, Kip1 ubiquitination-promoting complex protein 2; PPP1CB, Serine/threonine-protein phosphatase PP1-beta catalytic subunit; PTM, post-translational modification

* Corresponding author at: Animal Molecular and Cellular Biology group (AMCB), Louvain Institute of Biomolecular Science and Technology (LIBST), UCLouvain, Croix du sud 5, box L7.07.10, Louvain-la-Neuve 1348, Belgium.
E-mail address: rene.rezsohazy@uclouvain.be (R. Rezsohazy).

https://doi.org/10.1016/j.bbagrm.2019.07.005
Received 11 April 2019; Received in revised form 19 June 2019; Accepted 7 July 2019
Available online 16 July 2019
1874-9399/

Table 1
Primers used for plasmids construction.

	Forward (5′-3′)	Reverse (5′-3′)
attbKPC2	GGGGACAACTTTGTACAAAAAAGTTGGCATGTTCGTGCAGGAGGAGAAGAT	GGGGACAACTTTGTACAAGAAAGTTGGGTACGTGCGATTTAGTGTCTGG
KPC2ΔUBA_N-ter	GCGGCAGCTGCCGCAGAAGACCCGACCATAG	GGCAGCTGCCGCCTCGTCCAGCATTGCATTC
KPC2ΔUBA_C-ter	GCGGCAGCTGCCCGGAAGCCCTCTCCGGAG	GGCAGCTGCCGCAAACTCCCTTTTCCTCCGG
attbUbiquitinB	GGGGACAACTTTGTACAAAAAAGTTGGCATGCAGATCTTCGTGAAAAC	GGGGACAACTTTGTACAAGAAAGTTGGGACCACCTCTCAGACGCAG
Oligo6xHIS	CGATCATCACCATCACCATCACA	AGCTTGTGATGGTGATGGTGATGAT

inhibition. Nevertheless, beside TALE proteins, only a few HOX interactors have been identified so far. It can therefore be hypothesized that the amount of proteins influencing HOX activity is by far underestimated.

In order to identify new actors possibly involved in HOX activity regulation, we searched for candidate HOX interactors known to modulate target protein activities. We carried out a yeast two-hybrid screening involving the murine form of HOXA2 (mHOXA2) and the human ORFeome v3.1 [20,21]. HOXA2 is involved in hindbrain and cranio-facial development during mammalian embryogenesis. Further to this HOXA2 interactomic screening, we already described two novel interactions between HOXA2 and (1) RCHY1 (RING finger and CHY zinc finger domain-containing protein 1), an E3 ubiquitin ligase also known as PIRH2 [20,22], and (2) KPC2 (Kip1 ubiquitination-promoting complex protein 2), also known as UBADC1 [23]. With respect to RCHY1, we showed that mHOXA2 raises the proteasome-dependent degradation of RCHY1, but no apparent effect of RCHY1 on mHOXA2 activity has been highlighted so far [20,22]. For KPC2, Bridoux et al. provided evidence that it promotes the translocation of the human form of HOXA2 (hHOXA2) from the nucleus to the cytoplasm [23]. KPC2, in combination with KPC1, forms the Kip1 ubiquitination promoting complex (KPC). KPC1 is the catalytic subunit of this E3 ubiquitin ligase, whereas KPC2 is seen as a stabilizer of the complex and promotes the interaction between the proteasome and poly-ubiquitinated proteins, such as p27 [24,25]. While no apparent effect of KPC2 on hHOXA2 stability has been detected, the connection between KPC2, hHOXA2 ubiquitination and hHOXA2 relocation awaits for deeper investigation. Nonetheless, the hHOXA2 relocation in the presence of KPC2 has been correlated with a decline of mHOXA2 transcriptional activity promoted by KPC2 [23], providing new perspectives on HOX activity regulation by intra-cellular shuttling.

Here, we report a novel interaction between hHOXA2 and the beta catalytic subunit of the PP1 Ser/Thr phosphatase complex, namely PPP1CB. PP1 phosphatase complex is ubiquitous and conserved in all eukaryotes. PP1 is known to regulate a wide range of physiological functions such as transcription repression, pre-mRNA splicing, protein synthesis, cell cycle regulation, apoptosis, glycogen metabolism or synaptic transmission (reviewed in [26]). PP1 is a holoenzyme composed of a catalytic subunit (PPP1C) and a regulatory subunit (PPP1R or PIP for PPP1 interacting protein). While more than two hundred PPP1Rs have been reported in the literature, human PPP1Cs have been found to be encoded by three genes only, namely *Ppp1cα*, *Ppp1cβ* (also known as *Ppp1cδ*) and *Ppp1c*γ. These genes code for six isoforms obtained by alternative splicing: three for PPP1CA, one for PPP1CB and two for PPP1CC. All isoforms harbor a well conserved catalytic domain in PPP1C (~90% amino acid identity) but present a specific pattern of expression in terms of tissue localization, subcellular distribution and timing of expression (reviewed in [27]). PPP1CB is ubiquitously expressed but has been mainly characterized for its action on muscle contraction *via* its binding with the myosin phosphatase targeting protein (MYPT1), which acts as a PPP1R [28–30]. Interestingly, PPP1CB, in association with MYPT1, has been shown to induce a perinuclear relocation of the homeodomain-containing transcription factor NKX2.5 [31]. This translocation has further been correlated with a reduction of NKX2.5 transcriptional activity. Consistently, our study reveals that PPP1CB presents the ability to also regulate hHOXA2 activity. Strikingly, PPP1CB can functionally interact with KPC2 to modulate hHOXA2 activity, cellular localization, PTMs and stability. Therefore, our data support a model in which KPC2 and PPP1CB act together to regulate hHOXA2 protein activity.

2. Materials and methods

2.1. Plasmid construction

Gateway® expression (pExp) plasmids pExp-VN^{173}-hHOXA2 [23], pExp-FLAG-hHOXA2 [23], pExp-GST-KPC2 [23], pExp-VC^{155}-KPC2 [23], pExp-VN^{173} vectors for additional hHOX proteins [23], as well as plasmids pCS2-Prep1 [32], pCMV-PBX1a [33], pCMV-lacZ [34] and Hoxa2 r4-enhancer luciferase reporter [35] have been described elsewhere. Gateway® entry vector (pEnt) for PPP1CB was obtained from the hORFeome v3.1 (http://horfdb.dfci.harvard.edu) [21]. All proteins studied derive from human sequences. Expression vectors coding for HA-ubiquitin and 6xHis-ubiquitin were kindly provided by Yves Jossin (UCLouvain, IONS, Belgium) and Sonia Lain (University of Dundee, UK), respectively.

pEnt-KPC2ΔUBA_N-ter, pEnt-KPC2ΔUBA_C-ter, pEnt-KPC2ΔΔUBAs and pEnt-ubiquitin were generated using the Gateway® system from Invitrogen. BP-clonase® reactions for KPC2 mutants pEnt were achieved using pDONR223 vector and cDNA amplified by OE-PCR with specific primers (Table 1) on pEnt-KPC2 [23] vector. These pEnt plasmids were used in LR-clonase® reaction with pDest-GST N-ter [36] to generate pExp-GST-KPC2 mutants. BP-clonase® reaction for pEnt-Ubiquitin was achieved using pDONR223 vector and cDNA amplified by PCR with specific primers (Table 1) on pHRSIN-6xHIS-ubi-GFP vector which was kindly provided by Michael H. Malim (King's College London, UK). This pEnt plasmid was used in LR-clonase® reaction with pDest-VN^{173} [37] to obtain pExp-VN^{173}-ubiqiuitin. pExp-GST-PPP1CB, pExp-VC^{155}-PPP1CB and pExp-VN^{173}-KPC2 were generated by LR-clonase® reaction using pEnt-PPP1CB or pEnt-KPC2 [23] with corresponding pDest: pDest-GST N-ter [36], pDest-VC^{155} [37] or pDest-VN^{173} [37]. pExp-6xHIS-hHOXA2 was obtained by substituting the FLAG tag by a HIS tag coding sequence (Table 1) in pExp-Flag-HOXA2 [23] plasmid. pExp-FLAG-$p27^{Kip1}$ was generated by LR-clonase® reaction using the pEnt-$p27^{Kip1}$ previously described [23] with pDest-FLAG N-ter ™ [37].

2.2. Two-hybrid screening

The yeast two-hybrid screening for the murine form of HOXA2 was performed as previously described [20].

2.3. Cell culture, transfection and treatments

Human embryonic kidney (HEK293T) and African green monkey kidney fibroblast-like (COS7) cell lines were maintained in culture flasks at 37 °C under 5% of CO_2. D-MEM medium (Gibco, Hek293T: #61965-059; COS7: #31885-023) was supplemented with 10% fetal albumin serum (Invitrogen, #10270-106) and 100 U/ml penicillin-strepomycin (Gibco, #15140-122). HEK293T cell medium was supplemented with 1 mM sodium pyruvate (Gibco, #11360-070). Unless otherwise stated, HEK293T cells were plated on 6-well plates from suspensions at 350,000 cells/ml, 2 ml per well. COS7 cells were plated

on glass coverslips in 24-wells plates from suspensions at 100,000 cells/ml, 1 ml per well. Twenty-four hours after plating, cells at 50% of confluence were transfected with specific plasmid constructions (see each section for details) using JetPrime transfection reagent (Polyplus-transfection, #114-07). For cell treatment with drugs, cells were plated on wells coated with 0.01 mg/ml poly-D lysine hydrobromide in PBS (Sigma, #P7405). For proteasome inhibition, HEK293T cells were treated 32 h after transfection with 6.6 μM MG132 (Calbiochem, #474790) dissolved in DMSO, or with DMSO as control, during 16 h. For half-life analysis, HEK293T cells were treated 24 h after transfection with 200 μg/ml cycloheximide (Sigma, #01810) dissolved in DMSO, or with DMSO as control, during up to 4.5 h. For PP1 inhibition, HEK293T cells were treated 48 h after transfection with 5–10 nM Calyculin A (Santa Cruz Biotechnology, sc-2400) dissolved in DMSO, or with DMSO as control, during 1 h.

2.4. Antibodies

Antibodies were used as follows. For western blotting, the primary antibodies mouse anti-FLAG antibody (Sigma, #F1804), mouse anti-GST antibody (Sigma, #G1160), rabbit anti-H3S10Ph (Abcam, ab5176), mouse anti-STAT3 (pS727.25) (Santa Cruz Biotechnology, sc-293059) and HRP-coupled mouse anti-β-ACTIN antibody (Sigma, #A3854) were diluted at 1/5000, 1/5000, 1/2000, 1/2000 and 1/20,000, respectively, in 1% milk TBS (1 mM Tris, 155 mM NaCl, pH 7.5) 0.1% in Tween20 (TBS-T). For western blotting, the secondary antibodies anti-m-IgGκ BP-HRP (Santa Cruz Biotechnology, sc-516102) and anti-rabbit IgG-HRP (Santa Cruz Biotechnology, sc-2370) were diluted both at 1/10,000 in TBS-T.

For immuno-fluorescence the primary antibodies mouse anti-FLAG antibody (Sigma, #F1804), mouse anti-GST antibody (Sigma, #G1160) and rabbit anti-HOXA2 antibody (Sigma, #H9665) were diluted at 1/100, 1/200 and 1/100, respectively, in 1% milk TBS-0.1% in TritonX100 (T-TBS). For immunofluorescence, the secondary antibodies anti-mouse AlexaFluor® 555 (Invitrogen, #A-31570), anti-mouse AlexaFluor® 488 (Cell Signaling, #4408) and anti-rabbit AlexaFluor® 555 (Cell signaling, #4413S) antibodies were all diluted at 1/500 in T-TBS.

2.5. In-situ hybridization (ISH) and RT-PCR on mouse embryos

Sampling involving mice has been performed in accordance with the Animal Experimentation Ethics Committee of the UCLouvain (agreement number LA1220028) and in agreement with the European directive 2010/63/UE. Mice were maintained in a room at 21 °C under a 14 h/10 h light/dark cycle, with water and food in free access. Adult CD1 female and male were mated overnight. Females observed to have a post-coital plug the following morning (0.5 days) were euthanized by CO_2 inhalation ten days later (10.5 days) to collect embryos.

For ISH, embryos were collected on ice and fixed 15 min with 4% PFA in PBS at 4 °C. After three washes of 5 min in PBS, embryos were incubated 2-3 h with 30% sucrose in PBS at 4 °C, then covered with OCT Cryomatrix (Thermo Scientific, 6769006) and stored at −80 °C. 10 μm sagittal and transversal cryosections of embryonic day (E) 10.5 embryos were obtained by using Leica CM 3050S cryostat. Gene expression analysis by ISH was performed using the digoxigenin-labeled RNA probes procedure as previously described [38]. The *Ppp1cb* probe was designed against the murine sequence NM_172707.3 (Table 2, *Ppp1cb ISH probe*). For this purpose, pCR2.1-TOPO-PPP1CB was linearized with *Spe*I and probe was synthesized with T7 polymerase. The *Hoxa2* probe was obtained as described in [23]. Embryo sections were observed on a Leica DM2500 microscope and pictures were obtained with a Leica DFC420C camera.

For RT-PCR analysis, cDNA from embryos between E7.5 and E12.5 were collected as described [23]. *Ppp1cb*, *Hoxa2* and *Actin* were amplified with primers (PCR) listed in Table 2.

2.6. Protein co-precipitation

HEK293T cells were transfected with 300–500 ng of specific pExp plasmids encoding proteins fused with GST or FLAG, with a total of 1 μg of plasmid per condition. 48 h after transfection, cells were lysed with IPLS buffer (20 mM TrisHCl pH 7.5, 120 mM NaCl, 0.5 mM EDTA, 0.5% NP40, 10% glycerol) supplemented with Complete™ protease inhibitor (Roche, #11873580001) for 20 min with agitation on ice. Cell lysate was centrifuged 5 min at 16,000*g*, 4 °C. 30 μl of GST-beads (Sigma, #GE17-0756-01) reconditioned in cold IPLS buffer were added to 200 μl of cell lysate and incubated overnight (O/N) at 4 °C on a rotating wheel. Beads were then washed with 150 μl of cold IPLS buffer and centrifuged 5 min at 500*g* 4 °C. Washing step was achieved 3× and beads were finally mixed to 60 μl Laemmli 2× in IPLS, boiled 5 min at 95 °C and run on a 10% SDS-PAGE gel. Western blotting was used to visualize GST- and FLAG-tagged proteins, as well as ACTIN.

2.7. Biomolecular fluorescence complementation (BiFC) and immunofluorescence

COS7 cells were transfected with 150–250 ng of specific pExp-VN^{173} and pExp-VC^{155} plasmids coding for fusion proteins. Construction encoding FLAG or GST-tagged proteins were added in combination with a total of 800 ng of plasmid per condition. 24 h after transfection, cells were washed 2 × 5min with PBS then fixed on the coverslips with 4% PFA (Sigma, #441244) in PBS. Coverslips were then washed 2 × 5min with TBS buffer (50 mM Tris, 155 mM NaCl, pH 7.5) 0.1% in TritonX100 (Sigma, #10789704001) (T-TBS), 1 × 5min with TB buffer (50 mM Tris pH 7.5) and mounted on microscope slides with mounting medium complemented with DAPI (Labconsult, VEC·H-1200).

For immunofluorescence, after fixation and washing steps, coverslips were blocked 30 min with T-TBS 10% in non-fat milk. Suitable primary antibodies were then incubated O/N on coverslips in T-TBS 1% in non-fat milk. Coverslips were then washed 3 × 5min whit T-TBS and incubated 1 h with secondary antibody in T-TBS. Coverslips were then washed 2x5min with T-TBS, 1 × 5min with TB buffer and mounted as above.

Pictures were taken under epifluorescence microscope (Axioskop 2, Zeiss) and confocal microscope (LSM 710). For Bimolecular Fluorescence Complementation (BiFC), green fluorescent signal was quantified using ImageJ software and the experiment was considered as valid when signal intensity for a BiFC was three times higher than those obtained for negative controls.

Table 2
Primers used for ISH and RT-PCR.

	Forward (5′-3′)	Reverse (5′-3′)	Tm (°C)	Size (bp)
Ppp1cb ISH probe	AGTCTGGTGCCGACAAGATG	TCAGGTACGTCAGTGGGTCT	65	604
Ppp1cb PCR	GAGACCCACTGACGTACCTG	GTGGATTAGCTGTTCGAGGC	55	404
Hoxa2 PCR	AGACCTCGACGCTTTCACAC	TGGTTTTCCTTGCACTGGGT	55	499
Actin PCR	CCACCATGTACCCAGGCATT	AGGGTGTAAAACGCAGCTCA	57	253

2.8. Luciferase assay

HEK293T cells were plated on 24-wells plates from suspensions at 150,000 cells/ml, 1 ml per well. Cells at 50% confluence were transfected with 25–250 ng of specific plasmids containing *LacZ* and *HRE* reporters and with plasmids coding for PREP1, PBX1A, FLAG-hHOXA2 and interactors fused with GST. An empty GST coding plasmid was added to reach a total of 500 ng of plasmid in each condition. Each condition was assayed in triplicate. 48 h after transfection, cells were lysed using 250 µl of Lysis Reagent from the B-Gal Reporter Gene Assay kit (Roche, #11758241001) for 20 min with agitation. This kit was used in combination with Luciferase Reporter Gene Assay kit (Roche, #11669893001). Relative transcriptional activity of HOXA2 was quantified by the luminometric measurement of Luciferase (Luc) activity reported on Galactosidase (Gal) activity.

2.9. Ni-NTA column

HEK293T cells were transfected with 300–500 ng of specific pExp plasmids coding for FLAG-hHOXA2, HA-ubiquitin, 6xHIS-ubiquitin and interactors or KPC2 mutants fused with GST, with a total of 1 µg of plasmid per condition. 32 h after transfection, cells were treated O/N with 6.6 µM MG132. 48 h after transfection, cells were lysed with Guanidium 6 M buffer (6 M Guanidium Hydrochloride, 500 mM NaCl, 20 mM Na_2HPO_4/NaH_2PO_4, pH 7.8) supplemented with Complete™ protease inhibitor (Roche, #11873580001) for 20 min with agitation on ice. 50 µl of Ni-NTA agarose beads (Qiagen, #30210) were washed 2× with MiliQ H_2O and 2× with denaturing buffer (8 M Urea, 500 mM NaCl, 20 mM Na_2HPO_4/NaH_2PO_4, pH 7.8) supplemented with 20 mM Imidazole. 200 µl of agarose beads in denaturing buffer were added to 200 µl of cell lysate and incubated 30 min at RT on a rotating wheel. Agarose beads were then centrifuged 2 min at 1000*g* 4 °C and washed 2× with 400 µl of denaturing buffer-pH 7.8–20 mM Imidazole, 2× with 400 µl of washing buffer (8 M Urea, 500 mM NaCl, 20 mM Na_2HPO_4/NaH_2PO_4, pH 6) 20 mM Imidazole and 2× with 400 µl of washing buffer-pH 5.3–20 mM Imidazole. Agarose beads were finally mixed to Laemmli 2× in IPLS, boiled 5 min at 95 °C and run on a 10% SDS-PAGE gel. Western blotting was used to visualized GST and FLAG-tagged proteins, as well as ACTIN.

2.10. Half-life analysis

HEK293T cells were transfected with 300–500 ng of specific pExp plasmids coding for FLAG-hHOXA2 and interactors or KPC2 mutants fused with GST, with a total of 1 µg of plasmid per condition. 24 h after transfection, cells were treated with 200 µg/ml of cycloheximide for up to 4.5 h. Each 1.5 h, cells were lysed with IPLS buffer (20 mM TrisHCl pH 7.5, 120 mM NaCl, 0.5 mM EDTA, 0.5% NP40, 10% glycerol) supplemented with Complete™ protease inhibitor (Roche, #11873580001) for 20 min with agitation on ice. Cell lysate was centrifuged 5 min at 16,000*g*, 4 °C. 50 µl of each lysate were mixed to Laemmli 6×, boiled 5 min at 95 °C and run on a 10% SDS-PAGE gel. Western blotting was used to visualize GST and FLAG-tagged proteins, as well as ACTIN. ImageJ software was used to estimate protein abundance.

2.11. Phosphatase assay

HEK293T cells were transfected with 500 ng of specific pExp plasmids coding for FLAG-hHOXA2 and GST or PPP1CB-GST, with a total of 1 µg of plasmid per condition. 48 h after transfection, cells were treated 1 h with 10 nM of Calyculin A and lysed with IPLS buffer for 20 min with agitation on ice. Cell lysate was centrifuged 5 min at 16,000*g*, 4 °C. 50 µl of input were mixed to Laemmli 6×, boiled 5 min at 95 °C and run on a 10% SDS-PAGE gel. Western blotting was used to visualize GST and FLAG-tagged proteins, as well as ACTIN in the input samples. 35 µl of lysate were then incubated 1 h30 at 37 °C with 295 µl of Phosphatase buffer (25 mM Tris-HCL pH 7.9, 10 mM $MgCl_2$, 1 mM DTT, 100 mM NaCl, 1% TritonX100) supplemented with Complete™ protease inhibitor and 20 U of rAPid Alkaline Phosphatase (Sigma, #4898133001). As a control, 35 µl of lysate were incubated 1 h30 at 37 °C with 315 µl of Phosphatase buffer without rAPid Alkaline Phosphatase. 50 µl of each mix were mixed to Laemmli 6×, boiled 5 min at 95 °C and run on a 10% SDS-PAGE gel. Western blotting was used to visualize FLAG-tagged proteins, as well as ACTIN in the output samples.

2.12. Mass spectrometry analysis

HEK293T cells were transfected with 1 µg of pExp-6xHIS-hHOXA2. 32 h after transfection, cells were treated O/N with 6.6 µM MG132. 48 h after transfection, cells were treated with 6.6 µM MG132 and 5 nM Calyculin A or DMSO for 1 h. Cells were lysed with Guanidium 6 M buffer (6 M Guanidium Hydrochloride, 500 mM NaCl, 20 mM Na2HPO4/NaH2PO4, pH 7.8) supplemented with 0.5 mM PMSF for 20 min with agitation on ice. 100 µl of Ni-NTA agarose beads were washed 2× with MiliQ H_2O, 2× with denaturing buffer (8 M Urea, 500 mM NaCl, 20 mM Na_2HPO_4/NaH_2PO_4, pH 7.8) supplemented with 10 mM Imidazole. 400 µl of agarose beads in denaturing buffer were added to 400 µl of cell lysate and incubated O/N at 4 °C on a rotating wheel. Agarose beads were then centrifuged 2 min at 1000*g* 4 °C and washed 2× with 400 µl of denaturing buffer-10 mM Imidazole. 6xHIS-tagged proteins were eluted with 200 µl of Native buffer (500 mM NaCl, 50 mM Na_2HPO_4/NaH_2PO_4, pH 8) supplemented with 200 mM Imidazole. 50 µl were used in Western blotting to check HOXA2 purification and 150 µl were quick frozen and stored at −80 °C for mass spectrometry analysis.

Samples were first reduced in presence of 10 mM DTT for 30 min at 56 °C and then alkylated with 60 mM Chloroacetamide for 30 min at 22 °C in the dark. Both incubations were made under 500 rpm shaking condition. Samples were then precipitated by the addition of 4 volumes of Methanol and 1 volume of Chloroform. Both stock solutions being kept at −20 °C. Samples were vortexed 30 s before being incubated on ice for 20 min. Samples were centrifuged 15 min at 20,000 *g* at 4 °C. After removal of the upper phase, samples were mixed with 1.6 ml of pre-chilled Methanol by gentle tube inversion and incubated on ice for an additional 5 min before being centrifuged 15 min at 20,000 *g* at 4 °C. After removal of the supernatant, pellets were dried in a SpeeVac vaccum system before being resuspended in 200 µl of 200 mM TEAB (TrieEthylAmonium Bicarbonate) pH 8.0. Samples were digested overnight at 37 °C by adding 1.5 µl of Trypsin/lysC (Promega, #V5071). Digestion was stopped by adjunction of 10 µl of 10% TFA (Trifluoroacetic acid) before being raised to dryness with a SpeedVac vacuum system. Samples were recovered in 50 µl of 3.5% Acetonitrile (ACN)-0.1% TFA. Peptides concentration was determined by the use of Pierce™ Quantitative Colorimetric Peptide Assay (Thermo Scientific, #23275), according to manufacturer's instructions. At the end, samples were adjusted to 0.12 µg/µl with 3.5% ACN-0.1% TFA.

Peptides were then dissolved in solvent A (0.1% TFA in 2% ACN), directly loaded onto reversed-phase pre-column (Thermo Scientific, Acclaim PepMap 100) and eluted in backflush mode. Peptide separation was performed using a reversed-phase analytical column (Thermo Scientific, Acclaim PepMap RSLC, 0.075 × 250 mm) with a linear gradient of 4%–36% solvent B (0.1% TFA in 98% ACN) for 36 min, 40%–99% solvent B for 10 min and holding at 99% for the last 5 min at a constant flow rate of 300 nl/min on an Ultimate 3000 RSLN nanoHPLC system (Thermo Scientific). The peptides were analyzed by an Orbitrap Fusion Lumos tribrid mass spectrometer (ThermoFisher Scientific). The peptides were subjected to nanospray ionization source followed by tandem mass spectrometry (MS/MS) in Fusion Lumos coupled online to the UPLC. Intact peptides were detected in the Orbitrap at a resolution of 120,000. Peptides were selected for MS/MS using HCD setting at 35 and CID at 30 with multistage activation for neutral loss of phosphoric acid (97.976 Da); ion fragments were

detected in the Ion trap. A data-dependent procedure of MS/MS scans was applied for the top precursor ions above a threshold ion count of 5.0E3 in the MS survey scan with 30.0 s dynamic exclusion. The total cycle time was set to 4 s. MS1 spectra were obtained with an AGC target of 4E5 ions and a maximum injection time of 50 ms, and MS2 spectra were acquired with an AGC target of 1E4 ions and a maximum injection time of 35 ms. For MS scans, the *m/z* scan range was 350 to 1800. The resulting MS/MS data was processed using Sequest HT search engine within Proteome Discoverer 2.2 against a human protein reference database obtained from Uniprot. Trypsin was specified as cleavage enzyme allowing up to 2 missed cleavages, 4 modifications per peptide and up to 3 charges. Mass error was set to 10 ppm for precursor ions and 0.1 Da for fragment ions. Oxidation on Met, phosphorylation on Ser, Thr and Tyr were considered as variable modifications. False discovery rate (FDR) was assessed using Percolator and thresholds for protein, peptide and modification sites were specified at 1%. Phosphorylation sites were assigned by ptmRS node 2.0 and manually validated.

2.13. Statistical analysis

Statistical analyses for HOXA2 relocation and transcriptional activity were performed using JMP or SAS software. General linear model was used with experiment as a random parameter and relocation or activity data as a fix parameter. Bonferroni-Sidak correction was applied for multiple comparisons.

3. Results

3.1. Identification of PPP1CB, a catalytic subunit of the PP1 phosphatase, as a novel hHOXA2 interactor

In order to identify new HOXA2 interactors, a yeast two-hybrid screening was initially performed against the hORFeome v3.1 using mHOXA2, both as bait and prey [20,21]. Among the 10.214 human proteins represented in this library, more than a hundred potential mHOXA2 interactors were identified. As HOXA2 activity regulation is poorly studied, we decided to focus on the interaction between HOXA2 and PPP1CB, a catalytic subunit of the PP1 phosphatase complex known to regulate the homeodomain transcription factor NKX2.5 [31]. PPP1CB sequence is 100% identical between mouse and human proteins, while the mouse and human HOXA2 proteins are 94.4% identical. We therefore started by addressing if the human form of hHOXA2 also interacted with PPP1CB.

To validate whether the human form of HOXA2 also interacted with PPP1CB, co-precipitation (CoP) was performed in human embryonic kidney (HEK293T) cells transfected with plasmids coding for hHOXA2 fused with a FLAG tag (FLAG-hHOXA2) and PPP1CB fused with Glutathione S-transferase (GST) (GST-PPP1CB). As a control, FLAG-hHOXA2 was co-transfected with an unfused GST. After lysis, protein fractions were incubated with glutathione-sepharose beads and GST proteins were pulled down. The presence of FLAG-hHOXA2 in pull-down fractions was observed by western blotting. Our results revealed that FLAG-hHOXA2 is only pulled-down when GST-PPP1CB is expressed, suggesting interaction between PPP1CB and hHOXA2 (Fig. 1A). This result corroborates the interaction revealed by the yeast two-hybrid method.

In order to characterize this interaction, we decided to visualize the PPP1CB-hHOXA2 interaction by Bimolecular Fluorescence Complementation (BiFC) assay. To that end, African green monkey kidney fibroblast-like (COS7) cells were transfected with plasmids coding for hHOXA2 and PPP1CB fused with the N-terminal part (VN^{173}-hHOXA2) or the C-terminal part (VC^{155}-PPP1CB) of the VENUS protein, respectively. If HOXA2 and PPP1CB interact, VN^{173} and VC^{155} parts complement to reconstitute the VENUS protein and a green fluorescent signal can be observed under the microscope. To discriminate the signal provided by the interaction from background reassembly of the VENUS, negative controls were obtained by transfecting each fusion protein with its complementary unfused VN^{173} or VC^{155} VENUS moiety (Suppl. Fig. 1A). An interaction signal was considered to be valid if its intensity was at least three times higher than the background provided by controls (Suppl. Fig. 1B). As shown in Fig. 1B, the PPP1CB-hHOXA2 interaction generated a BiFC signal restricted to a small proportion of the cytoplasm, as well as some dots in the nucleus.

We then asked whether the interaction with PPP1CB could define a generic property shared by other HOX proteins. BiFC assays were repeated with hHOX proteins belonging to distinct paralogous groups and we showed that PPP1CB could interact with all proteins tested, namely HOXA1, HOXB1, HOXB2, HOXB5, HOXC11 and HOXD10 (Suppl. Fig. 2). Nonetheless, it is worth mentioning that distinct interaction patterns were observed depending on the hHOX protein tested. PPP1CB interaction with HOXA1, HOXB5 and HOXD10 showed indeed a predominantly nuclear signal, while PPP1CB-HOXB1, HOXB2 and HOXC11 presented a predominantly cytoplasmic signal. These observations support that the ability to interact with PPP1CB could be well conserved among hHOX proteins. However, since interactions gave rise to different BiFC patterns, PPP1CB interactions might display distinct functional outcomes according to each hHOX protein.

Taken together, our results indicate that PPP1CB can interact with multiple hHOX proteins. In this report, we subsequently focused on hHOXA2, whose interaction with PPP1CB appears located in both cytoplasm and nucleus.

3.2. Ppp1cb expression overlaps with Hoxa2 activity during mouse embryogenesis

To address whether the PPP1CB-HOXA2 interaction might take place during embryonic development, we characterized the expression pattern of *Ppp1cb* during mouse embryogenesis and compared it with that of *Hoxa2*. As *Hoxa2* activity has been shown to be critical between 8.5 days (E8.5) and 12.5 days (E12.5) post-fertilization in the mouse embryo [39,40], we investigated if *Ppp1cb* is expressed during this period of time. We first analyzed *Ppp1cb* expression by RT-PCR from whole mouse embryos at different stages of development and showed that *Ppp1cb* is continuously expressed between E8.5 and E12.5 (Fig. 2A). Next, *In Situ* Hybridizations (ISH) against *Ppp1cb* and *Hoxa2* mRNAs were carried out on serial sagittal and transverse sections of E10.5 mouse embryos (Fig. 2B–C). *Ppp1cb* appeared to be ubiquitously expressed in the E10.5 mouse embryo (Fig. 2B). Notably, *Ppp1cb* is expressed in the second branchial arch (BAII) (Fig. 2C, images i–iv), which is an embryonic structure whose patterning critically relies on HOXA2 [39,40]. *Ppp1cb* is also expressed in the hindbrain where *Hoxa2* is active. However, while *Hoxa2* expression in the rhombencephalon extends rostrally up to the boundary between the rhombomeres (r) 1 and r2, *Ppp1cb* is expressed in the entire rhombencephalon including r1 (Fig. 2C, images v and vi).

To sum up, these observations show that *Ppp1cb* and *Hoxa2* expression overlap in time and space in territories where *Hoxa2* fulfills important functions in the mouse embryo. This supports that the PPP1CB-HOXA2 interaction can occur *in vivo*.

3.3. hHOXA2, PPP1CB and KPC2: a functional trio in interaction?

We noticed that the cellular BiFC signal for the PPP1CB-hHOXA2 interaction was quite similar to the BiFC interaction pattern previously highlighted for the interaction between HOXA2 and the ubiquitin-ligase adapter protein KPC2 [23], including large dots in the nucleus and a cytoplasmic labeling. Interestingly, both PPP1CB and KPC2 have been described to modulate transcription factor intra-cellular distribution [23,31]. In addition, PPP1CC isoforms were reported to interact with the E3 ubiquitin ligase SIAH2 in rat brain [41], suggesting that phosphatase and ubiquitin ligase complexes could functionally interplay.

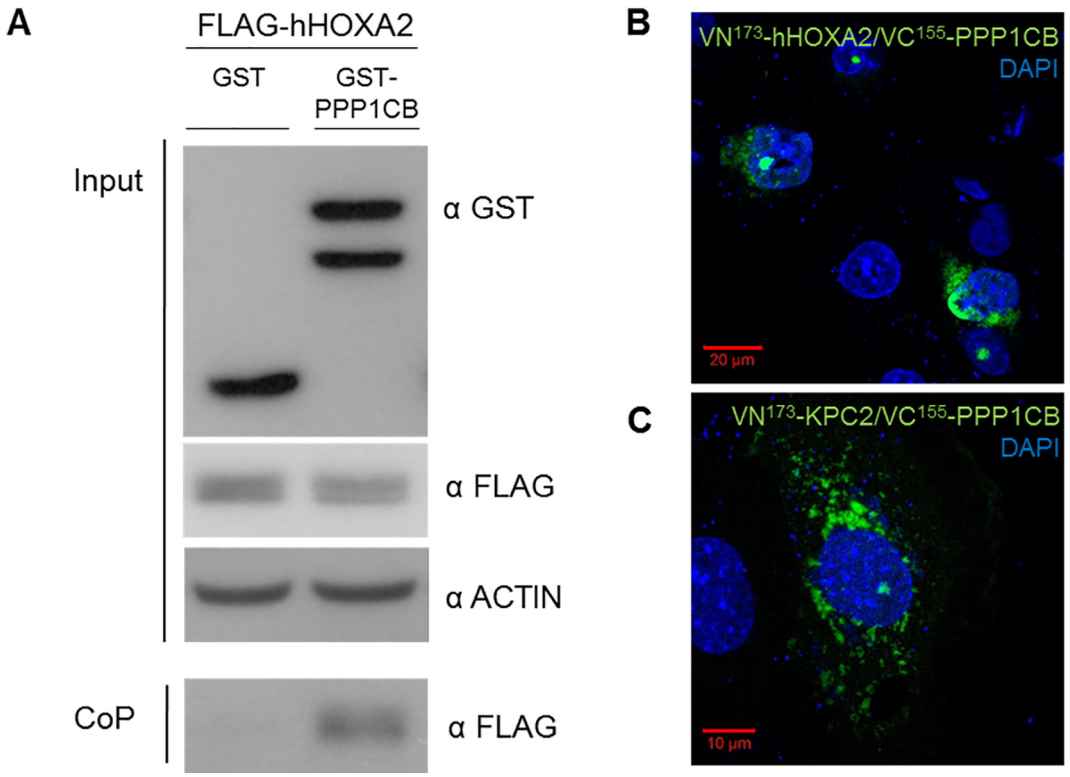

Fig. 1. PPP1CB interacts with hHOXA2 and KPC2. A: Co-precipitation (CoP) assay. HEK293T cells were transfected with a combination of pExp plasmids coding for FLAG-hHOXA2, GST and GST-PPP1CB. Proteins were detected by western blotting before (Input) and after (CoP) co-precipitation on glutathione beads which bind GST tag. Antibodies were directed against GST or FLAG tags. β-ACTIN detection was used as control. ($N > 3$) B and C: Bimolecular fluorescence complementation (BiFC). COS7 cells were transfected with pExp plasmids coding for VC^{155}-PPP1CB and VN^{173}-hHOXA2 (B) or VN^{173}-KPC2 (C) in combination. BiFC signal shows protein interaction in green. Nuclei were stained with DAPI (blue). Pictures were taken under confocal microscope. Scale bars = 10 µm. ($N \geq 3$). (For interpretation of the references to colour in this figure legend, the reader is referred to the web version of this article.)

We therefore tested whether PPP1CB and KPC2 could also interact. Both BiFC and CoP assays confirmed PPP1CB-KPC2 interaction (Fig. 1C, Suppl. Fig. 3). In addition, the BiFC signal revealed a predominantly cytoplasmic interaction.

On the basis of the BiFC results, we next investigated whether all three proteins, hHOXA2, PPP1CB and KPC2, could co-localize –at least partly- in the cell. In order to study the subcellular localization of each partner upon interaction, COS7 cells were transfected with two different combinations of plasmids: (1) VN^{173}-hHOXA2, VC^{155}-PPP1CB and GST-KPC2, and (2) VN^{173}-hHOXA2, VC^{155}-KPC2 and GST-PPP1CB (Fig. 3). We next visualized the BiFC signal obtained upon interaction between two partners, coupled to immunofluorescence detection of the third protein tagged with GST. To address whether all three proteins could establish tripartite interactions, we determined whether BiFC between two partners could at least partly trap the third interactor. Our results revealed a clear cytoplasmic co-localization of KPC2 together with the interacting PPP1CB-hHOXA2 and of PPP1CB with KPC2-hHOXA2. To a lesser extent, a weak co-localization can be observed in the nucleus.

Taken together, these results support that hHOXA2, KPC2 and PPP1CB can form a trio of interacting proteins possibly exerting mutual influences.

3.4. HOXA2 transcriptional activity is modulated by PPP1CB and KPC2

By studying PPP1CB, our first idea was to analyze whether PPP1CB could regulate hHOXA2 activity like it does for NKX2.5 [31]. Interestingly, Bridoux et al. previously showed that KPC2 tends to decrease the transcriptional activity of mHOXA2 at a HOXA2-responsive element (HRE) [23]. To evaluate if PPP1CB and KPC2 could also influence the transcriptional activity of hHOXA2, HEK293T cells were transfected with plasmids coding for FLAG-hHOXA2 and GST-PPP1CB and/or GST-KPC2. Plasmids for the HOX cofactors PREP1 and PBX1A were added to promote a higher HOXA2 activity. The activity of hHOXA2 was evaluated through the activation of a target luciferase (*Luc*) reporter under the control of the previously characterized HRE [35]. As shown in Fig. 4, PPP1CB and KPC2 decreased the transcriptional activation provided by hHOXA2, whether they were expressed alone or conjointly. In addition, it appeared that PPP1CB also modified the activity mediated by PREP1 and PBX1A in the absence of hHOXA2. This observation prompted us to address whether PPP1CB could interact with PBX1A. BiFC experiments revealed that PBX1A could interact with PPP1CB, KPC2 and –as expected- hHOXA2 (Suppl. Fig. 4A). Furthermore, it appeared that all actors co-localized in the cytoplasm (Suppl. Fig. 4B). Immunofluorescence indeed revealed that (1) KPC2 co-localized with the PBX1A-PPP1CB interaction, (2) PPP1CB co-localized with the PBX1A-KPC2 interaction and (3) hHOXA2 co-localized in the cytoplasm with the PPP1CB-PBX1A interaction. As a control, no co-localization between FLAG-p27 and PBX1A-PPP1CB BiFC signal was observed, supporting that the co-localization between PPP1CB, KPC2, PBX1A and hHOXA2 is specific.

Taken together, these observations let us hypothesize that PBX1A and hHOXA2 could together be relocated or retained by PPP1CB and KPC2 in the cytoplasm. As a consequence, the protein shuttling induced by KPC2 and PPP1CB could influence hHOXA2 transcriptional activity directly and/or indirectly *via* PBX1A export in the cytoplasm.

3.5. PPP1CB and KPC2 induce hHOXA2 translocation from the nucleus to the cytoplasm

The fact that, like KPC2, PPP1CB could decrease HOXA2 transcriptional activity prompted us to determine if PPP1CB could also

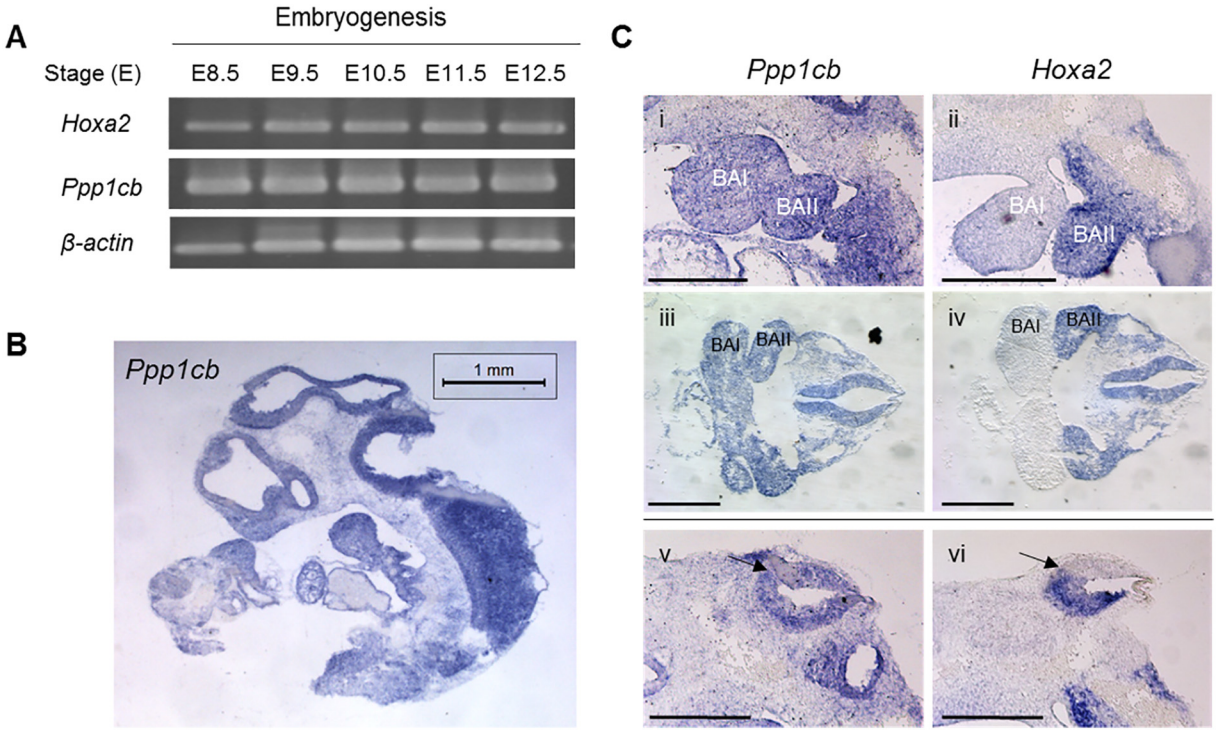

Fig. 2. *Ppp1cb* and *Hoxa2* show overlapping expression in the mouse embryo. A: RT-PCR. Detection of *Hoxa2* and *Ppp1cb* mRNA between E8.5 and E12.5 stages was achieved by RT-PCR on whole mouse embryo extract. *Actin* was used as a control. B and C: *In situ* hybridization (ISH). Expression of *Ppp1cb* gene was observed on sagittal sections of mouse embryo at E10.5 (B). Focus on *Ppp1cb* and *Hoxa2* gene expression in the branchial arches I (BAI) and II (BAII) (C, images i–iv), as well as in the rhombencephalon (C, images v–vi) of E10.5 mouse embryo in sagittal or transversal sections. Black arrows indicate the rhombomere (r)1/r2 boundary. Scale bars = 500 µm.

relocate HOXA2 in the cell. We indeed previously showed that KPC2 can induce hHOXA2 nuclear export through the receptor CRM1 and that this export was correlated with a decrease in HOXA2 activity [23]. Here, COS7 cells were transfected with two BiFC plasmid combinations, (1) VN^{173}-hHOXA2 and VC^{155}-PPP1CB with/without GST-KPC2, and (2) VN^{173}-hHOXA2 and VC^{155}-KPC2 with/without GST-PPP1CB (Fig. 5A). hHOXA2 localization was followed by immunofluorescence. The proportion of cells presenting a predominant hHOXA2 cytoplasmic

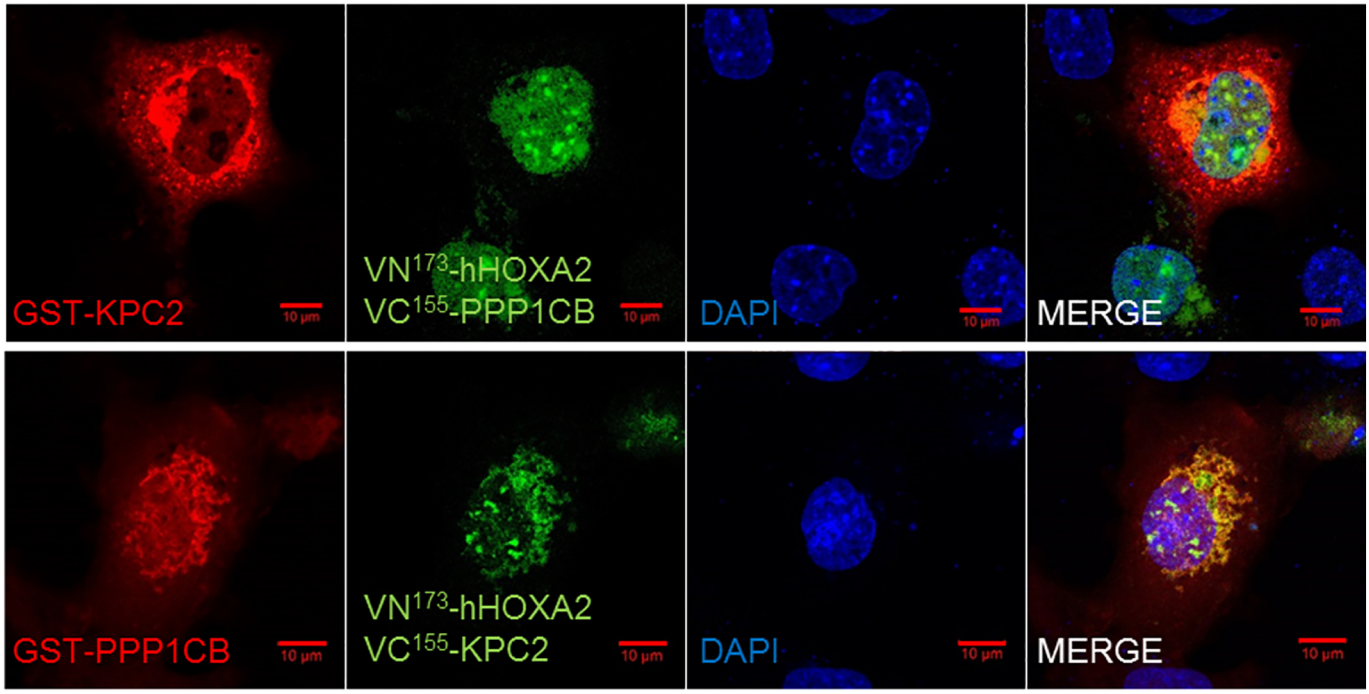

Fig. 3. hHOXA2, PPP1CB and KPC2 co-localize in the cytoplasm. COS7 cells were transfected with a combination of pExp plasmids coding for VN^{173}-hHOXA2, VC^{155}-PPP1CB, VC^{155}-KPC2, GST-KPC2 and GST-PPP1CB. BiFC signal (green) shows protein interaction. Red signal was observed after immunofluorescence against GST tag. Nuclei were stained with DAPI (blue). Pictures were taken under confocal microscope. Scale bars = 10 µm. (N = 3).

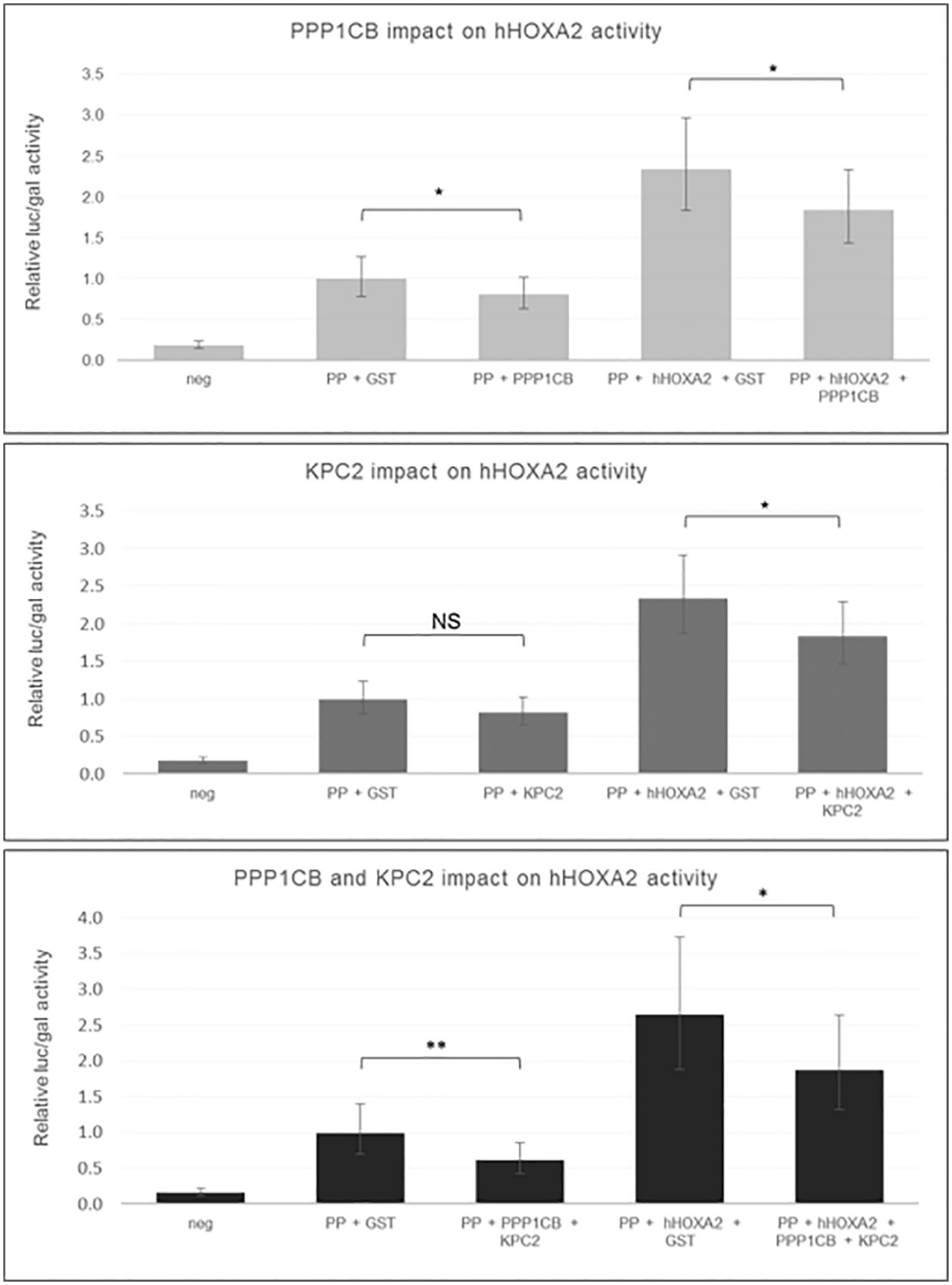

Fig. 4. PPP1CB and KPC2 decrease hHOXA2 transcriptional activity. HEK293T cells were transfected with two plasmids containing a *Luciferase* gene downstream a HOXA2 responsive element (HRE) and a *LacZ* reporter under the control of a CMV promotor. pExp plasmids coding for PREP1 and PBX1a (PP), FLAG-hHOXA2, GST, GST-PPP1CB (A and C) and GST-KPC2 (B and C) were added in combination to the transfection mix. Relative transcriptional activity of hHOXA2 was quantified by the luminometric measurement of Luciferase (Luc) activity reported to Galactosidase (Gal) activity. PP activation was set as a reference of '1'. NS = non-significant; *p-val $<$ 0.05; **p-val $<$ 0.01. Error bars = upper and lower intervals at 95%. (N = 6–10, n = 3).

signal (as illustrated on Fig. 5A, image close-up) was reported with respect to the total number of transfected cells (Fig. 5B). Such quantification revealed that when hHOXA2 interacted with PPP1CB upon BiFC, $<$ 15% of transfected cells showed a mostly cytoplasmic localization of hHOXA2, whether KPC2 was transfected or not. However, when hHOXA2 was in BiFC with KPC2, this proportion appeared significantly higher, reaching up to 30%. This result is in accordance with our previously published data [23]. Surprisingly, while PPP1CB was further added, the proportion of cells with mainly cytoplasmic hHOXA2 further increased, reaching up to 40%, showing that PPP1CB can contribute to enhance the cytoplasmic localization of hHOXA2. We therefore propose that hHOXA2 primarily interacts with KPC2 to be

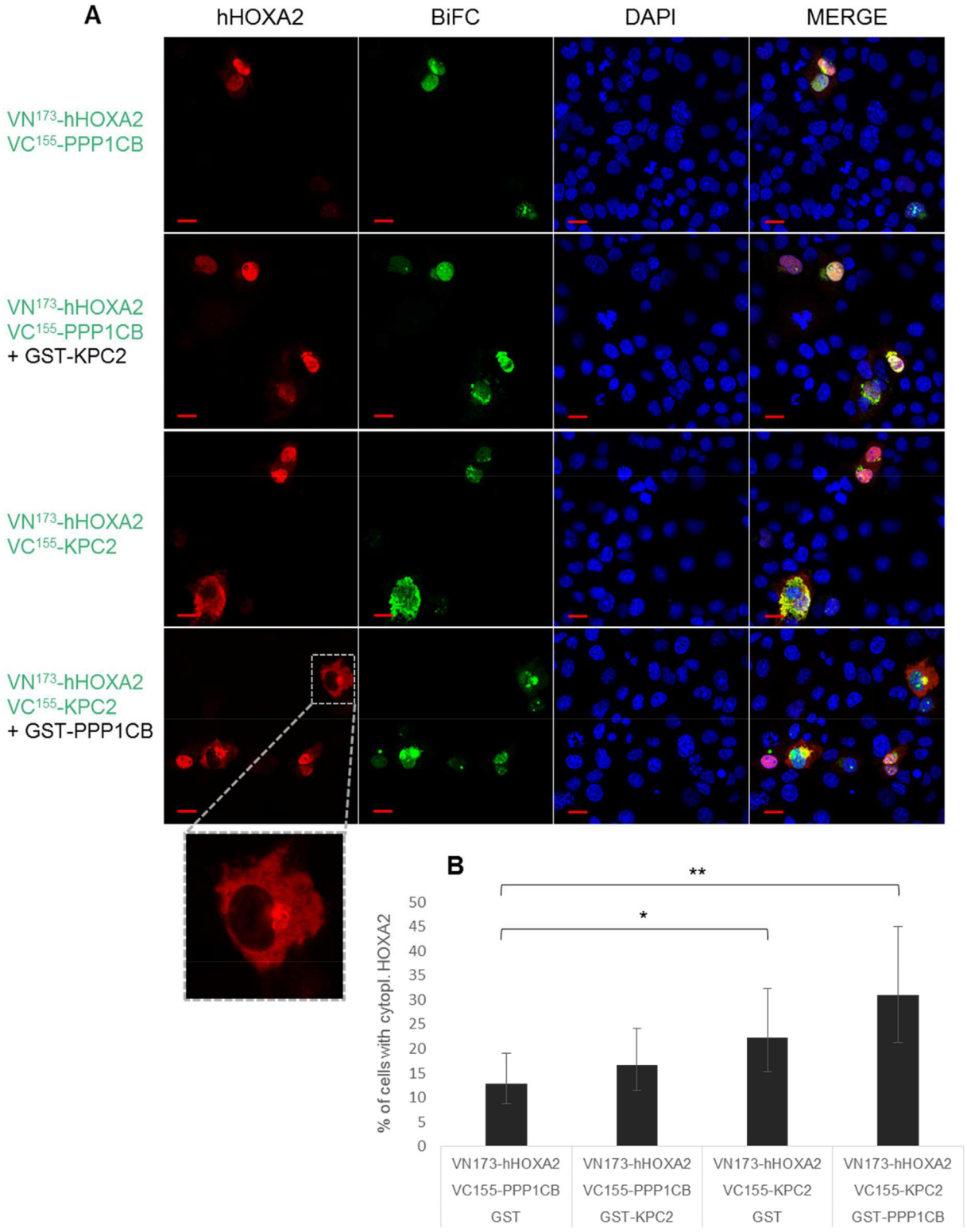

Fig. 5. KPC2 and PPP1CB relocate hHOXA2 in the cytoplasm. A: COS7 cells were transfected with a combination of pExp plasmids coding for VN^{173}-hHOXA2, VC^{155}-PPP1CB, VC^{155}-KPC2, GST, GST-KPC2 and GST-PPP1CB. BiFC signal (green) shows protein interaction. Red signal was observed after immunofluorescence against HOXA2. Nuclei were stained with DAPI (blue). Pictures were taken under confocal microscope. Scale bars = 20 μm. ($N > 3$) B: The percentage of cells presenting a mostly cytoplasmic HOXA2 (as highlighted in close-up: A, bottom picture, dotted frame) was reported on total transfected cells. ImageJ software was used to quantify the 'percentage of cells with cytoplasmic HOXA2'. Error bars = upper and lower intervals at 95%. *p-val < 0.05; **p-val < 0.01. ($N = 7$, $n = 3$).

transferred from the nucleus to the cytoplasm, and that cytoplasmic PPP1CB either enhances this transfer or promotes the cytoplasmic retention of HOXA2 while the three proteins interact together in the cytoplasm.

3.6. PPP1CB and KPC2 decrease the amount of ubiquitinated hHOXA2

Cellular trafficking and activity modulation are regularly subsequent to post-translational modifications (PTMs). As PPP1CB belongs

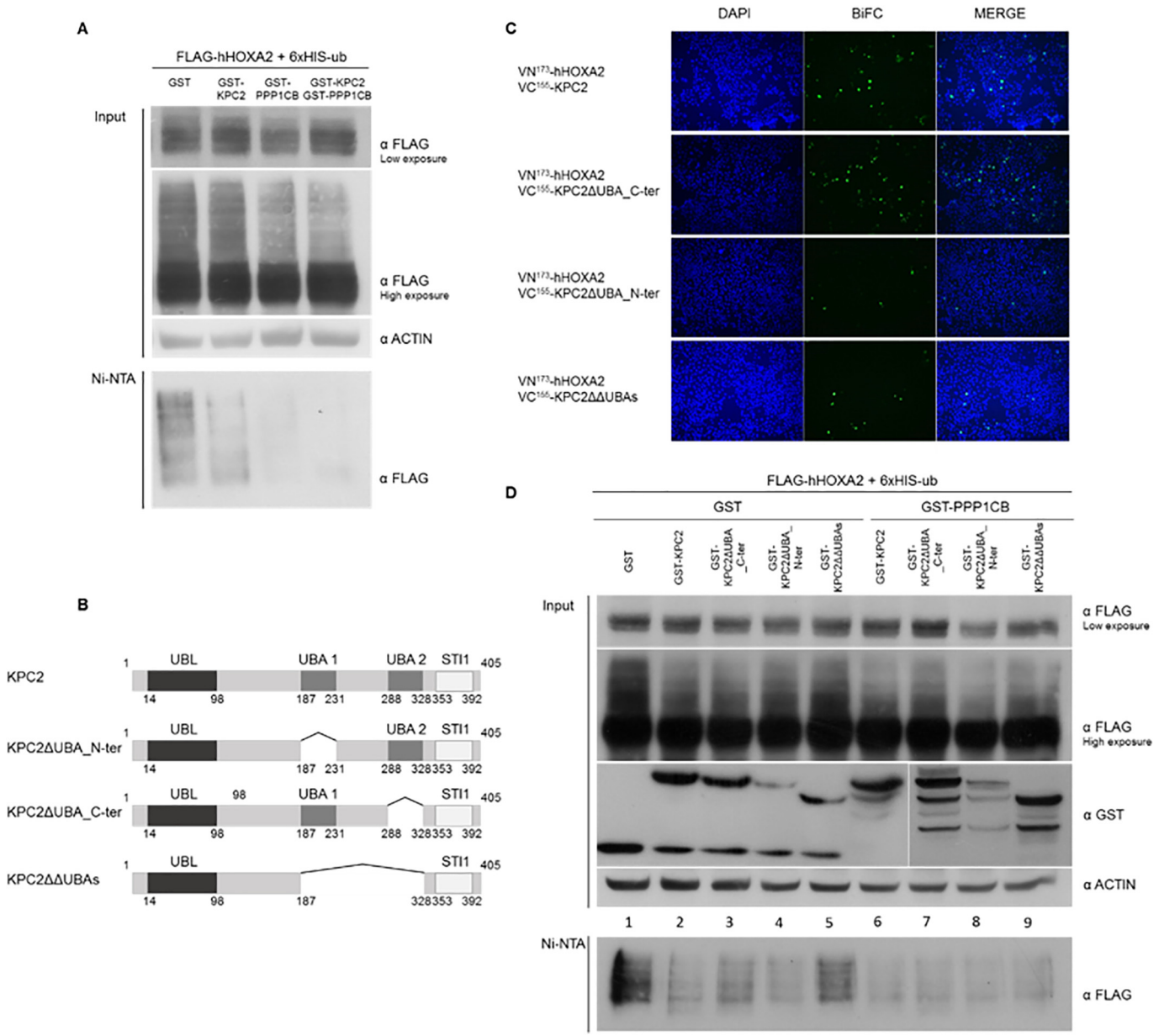

Fig. 6. PPP1CB and KPC2 are involved in a reduction of hHOXA2 ubiquitination. A: HEK293T cells were transfected with pCMV-6xHIS-ubiquitin and a combination of pExp plasmids coding for FLAG-hHOXA2, GST, GST-KPC2 and GST-PPP1CB. 36 h after transfection, cells were treated with 6.6 μM MG132. Abundance of hHOXA2 was analyzed by western blotting against FLAG before purification (Input). Purification of ubiquitinated proteins was carried out on an Ni-NTA affinity column. Abundance of ubiquitinated forms of hHOXA2 after Ni-NTA purification was analyzed by Western blotting against FLAG (Ni-NTA). β-ACTIN detection was used as a control. (N > 3) B: KPC2 UBA mutants. UBL = Ubiquitin-like domain; UBA = Ubiquitin associated domain; STI1 = Heat shock chaperonin-binding motif. C: For BiFC, COS7 cells were transfected with pExp plasmids coding for VN^{173}-hHOXA2 and VC^{155}-KPC2 or VC^{155}-KPC2 UBA mutants. BiFC signal (green) shows protein interaction. Nuclei were stained with DAPI (blue). Pictures were taken under epifluorescence microscope. (N = 3) D: HEK293T cells were transfected with pCMV-6xHIS-ub and a combination of pExp plasmids coding for FLAG-hHOXA2, GST, GST-PPP1CB, GST-KPC2, GST- KPC2ΔUBA_C-ter, GST- KPC2ΔUBA_N-ter and GST-KPC2ΔΔUBAs. 36 h after transfection, cells were treated with 6.6 μM MG132. Abundance of HOXA2 was analyzed by Western as in A. (N = 3).

to the PP1 Ser/Thr phosphatase complex and KPC2 belongs to an E3 ubiquitin ligase, interaction between hHOXA2 and these two partners could influence hHOXA2 PTM profile. We decided to start with ubiquitin analysis of hHOXA2. Ubiquitination can indeed impact physiological functions such as trafficking, degradation or nuclear translocation [42]. To address whether hHOXA2 is ubiquitinated and, if so, what could be the influence of both PPP1CB and KPC2 on hHOXA2 ubiquitination, HEK293T cells were transfected with plasmids coding for FLAG-hHOXA2, 6xHIS-ubiquitin and GST, GST-KPC2 and/or GST-PPP1CB (Fig. 6A). In order to inhibit HOXA2 proteasomal degradation, cells were treated with MG132, 12 h before protein analysis. Ubiquitinated proteins, tagged with the 6xHIS tag, were then purified through a Ni-NTA column. Proportion of ubiquitinated hHOXA2 (ub-hHOXA2) in each condition was then analyzed by western blotting. While the level of unmodified forms of hHOXA2 was similar in the presence or the absence of KPC2 and PPP1CB (Fig. 6A, “input”, “Low exposure”), we detected a clear reduction of ub-hHOXA2 when PPP1CB and/or KPC2 were expressed, with the strongest effect observed when PPP1CB was involved. These results show that both PPP1CB and KPC2 contribute to decrease the amount of ubiquitinated hHOXA2.

Previous studies highlighted that KPC2 is an adapter in ubiquitin ligase complexes. It interacts with poly-ubiquitinated proteins through two ubiquitin associated (UBA) domains [24,25]. In that regard, we aimed to determine if the decrease in ubiquitinated forms of hHOXA2

promoted by KPC2 and PPP1CB relies on these UBA domains. KPC2 mutants deleted for the N-terminal (KPC2ΔUBA_N-ter), the C-terminal (KPC2ΔUBA_C-ter) or both UBA domains (KPC2ΔΔUBAs) were generated (Fig. 6B). We first investigated if UBA domains are required for hHOXA2 interaction. COS7 cells were co-transfected with plasmids coding for VN^{173}-HOXA2 and VC^{155}-KPC2, VC^{155}-KPC2ΔUBA_C-ter, VC^{155}-KPC2ΔUBA_N-ter or VC^{155}-KPC2ΔΔUBAs. As observed in Fig. 6C, a BiFC signal appeared, with a similar intracellular pattern (Suppl. Fig. 5A), indicating a hHOXA2 interaction with wild-type KPC2 as well as with the three KPC2 deletion derivatives. It should be noted that the negative control expressing VN^{173} with VC^{155}-KPC2ΔUBA_N-ter provided a high fluorescence background which appeared with a similar intensity as with VN^{173}-hHOXA2 and VC^{155}-KPC2ΔUBA_N-ter. However, a closer examination at higher magnification clearly revealed that the negative control background BiFC pattern totally differed from the VN^{173}-hHOXA2/VC^{155}-KPC2ΔUBA_N-ter interaction pattern (Suppl. Fig. 5B). This supports that, despite a high background signal, HOXA2 still specifically interacted with KPC2ΔUBA_N-ter. Taken together, these data indicate that the UBA domains of KPC2 are not required for its interaction with hHOXA2.

To address the possible involvement of the UBA domains in the KPC2-mediated decrease in hHOXA2 ubiquitinated forms, 6xHis-tagged protein purification assays on Ni-NTA were repeated with GST-KPC2 mutants (Fig. 6D, lanes 1–5). After Ni-NTA column, we showed that hHOXA2 ubiquitination was slightly restored when C-terminal UBA domain was missing (Fig. 6D, lane 3). This restoration was clearly higher when both UBA domains were deleted (Fig. 6D, lane 5), showing a crucial role of these two domains in modulating the abundance of ub-hHOXA2. These results underlie that KPC2 might require UBA domains to promote the decrease in ub-hHOXA2. Surprisingly, when PPP1CB was expressed together with KPC2 mutants, no restoration of hHOXA2 ubiquitination could be observed (Fig. 6D lanes 6–9), *i.e.* the amount of ub-hHOXA2 decreased similarly in the presence of either mutant or the wild-type KPC2.

All together, these results show that KPC2 and PPP1CB reduce the abundance of the ubiquitinated forms of hHOXA2, presumably by deubiquitination. Indeed, loss of ub-HOXA2 cannot be due to HOXA2 proteasomal degradation as cells were treated with MG132. Alternatively, our results cannot exclude that PPP1CB and KPC2 impede HOXA2 ubiquitination. UBA domains of KPC2 are not involved in the interaction with hHOXA2 but are required for the reduction in ub-HOXA2. However, PPP1CB can compensate for the KPC2 loss of function when the UBA domains are deleted, in decreasing the amount of ub-HOXA2.

3.7. hHOXA2 half-life is affected by PPP1CB and KPC2

In the light of the loss of ub-hHOXA2 induced by KPC2 and PPP1CB, we wanted to determine whether this process could in turn stabilize hHOXA2. hHOXA2 half-life was measured in the presence of PPP1CB and/or KPC2. HEK293T cells were transfected with plasmids coding for FLAG-HOXA2 and GST, GST-KPC2 and/or GST-PPP1CB. Twenty-four hours after transfection cells were treated with cycloheximide (CHX) for up to 4.5 h to inhibit protein synthesis. The abundance of FLAG-hHOXA2 was then evaluated by western blotting between 0 and 4.5 h of CHX treatment (Fig. 7A). While PPP1CB slowly decreased the half-life of hHOXA2, KPC2 increased the stability of hHOXA2. This last observation is in line with the reduction of ubiquitinated forms of HOXA2 reported above. Interestingly, the effect of KPC2 prevailed over PPP1CB when proteins were expressed together. To address whether UBA domains are also involved in the KPC2-mediated stabilization of hHOXA2, hHOXA2 half-life was measured in the presence of KPC2 mutants (Fig. 7B). Quite significantly, hHOXA2 stabilization by KPC2 requires both UBA domains, whether PPP1CB is expressed or not. It is important to note that PPP1CB, KPC2 and KPC2 mutant proteins were stable between 0 and 4.5 h (Suppl. Fig. 6).

Therefore, PPP1CB and KPC2 display distinct but complementary effects on hHOXA2 regulation: they synergize in decreasing the abundance of ub-hHOXA2, but show opposed influence on hHOXA2 stability. PPP1CB, although promoting the hHOXA2 decay, is dominated by and cannot counteract the hHOXA2 stabilization mediated by KPC2 in a UBA-dependent manner. This in turn suggests that hHOXA2 stability is not directly correlated to its ubiquitination status.

3.8. Ubiquitin-hHOXA2 interaction co-localizes with PPP1CB and KPC2 in the cytoplasm

We saw earlier that PPP1CB, KPC2 and hHOXA2 can form a trio in the cytoplasm. Since PPP1CB and KPC2 influence the ubiquitination status of hHOXA2, we used BiFC to detect a possible interaction between HOXA2 and ubiquitin and to address whether this interaction could co-localize with the interactors KPC2 and PPP1CB. COS7 cells were transfected with two plasmid combinations: (1) VN^{173}-ubiquitin, VC^{155}-hHOXA2, GST-KPC2 and FLAG-PPP1CB; (2) VN^{173}-ubiquitin, VC^{155}-hHOXA2, GST-PPP1CB and FLAG-KPC2 (Fig. 8A). In order to analyze a possible co-localization with PPP1CB and KPC2, BiFC was combined with immunofluorescence detection of GST. Confocal pictures revealed that the ub-hHOXA2 interaction mainly takes place at specific locations in the nucleus. This interaction was also detected, although to a lesser extent, in the cytoplasm where the entire BiFC signal co-localized with KPC2 and PPP1CB. Interestingly, by differential protein extraction, we found that the ubiquitin-hHOXA2 interaction mainly located in the cell fraction containing histones and DNA (Suppl. Fig. 7), suggesting that ub-HOXA2 is associated to the chromatin. Taken together, these observations indicate that hHOXA2 interacts with ubiquitin at specific areas in the nucleus, probably in association with chromatin, or in the cytoplasm, where PPP1CB and KPC2 could compete with the nuclear location of ub-hHOXA2.

Finally, to address whether ubiquitin could be involved in hHOXA2 cytoplasmic shuttling, we analyzed the hHOXA2 cytoplasmic relocation when ubiquitin is overexpressed. To that end, a plasmid coding for HA-ubiquitin was transfected in combination with VN^{173}-hHOXA2, VC^{155}-KPC2 and GST-PPP1CB. As displayed on Fig. 8B, when ubiquitin is involved, the synergistic effect provided by KPC2 and PPP1CB on hHOXA2 cytoplasmic relocation is inhibited, supporting that ubiquitination retains hHOXA2 within the nucleus, where HOXA2 plays its role of transcription factor.

3.9. HOXA2 is targeted by PP1 phosphatase complex

Next, we studied hHOXA2 phosphorylation and addressed whether hHOXA2 can be a PP1 target. HEK293T cells were transfected with plasmids coding for FLAG-hHOXA2 and GST or GST-PPP1CB. Forty-eight hours after transfection, cells were treated 1 h with calyculine A (CalA), a strong inhibitor of PP1 and PP2A phosphatase activity. The concentration of CalA drug was adapted to inhibit only PP1 activity (Suppl. Fig. 8). HOXA2 modifications were revealed by western blotting. After CalA treatment, we observed new forms of hHOXA2 presenting a higher molecular weight than in untreated condition (Fig. 9A). To confirm these higher forms were phosphorylated proteins, protein samples were incubated with rAPid Alkaline Phosphatase for 1 h30. After incubation, the upper molecular weight forms of hHOXA2 observed upon CalA treatment disappeared, confirming that these forms are phosphorylated forms of HOXA2 (Fig. 9B).

In order to highlight hHOXA2 Ser/Thr sites targeted by PP1, mass spectrometry (MS) analysis was performed on either untreated HEK293T cells or those treated with CalA. Cells were transfected with plasmids for 6xHIS-hHOXA2 and treated thirty-six hours after transfection with MG132 for 12 h and, afterwards, with MG132 and CalA or DMSO for 1 h. Proteins were purified on Ni-NTA column and digested with trypsin before MS analysis. This revealed phospho-Ser and phospho-Thr residues in samples treated with DMSO (Fig. 9C) and CalA

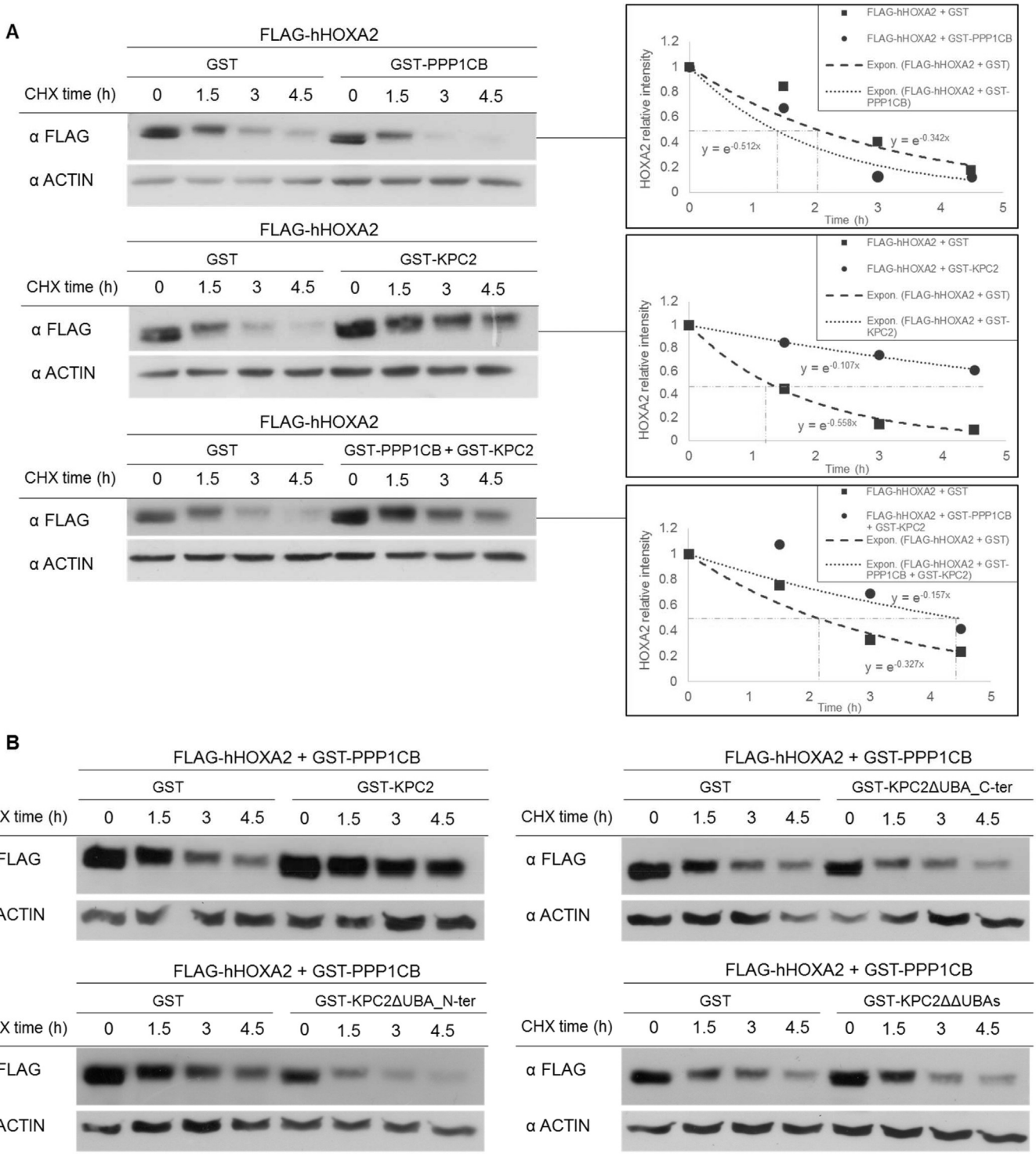

Fig. 7. KPC2 UBA domains are required for hHOXA2 protein stabilization. A: HEK293T cells were transfected with a combination of pExp plasmids coding for FLAG-hHOXA2, GST-KPC2, GST-PPP1CB and GST. In order to determine hHOXA2 half-life, cells were treated 24 h after transfection with 200 μg/ml of cycloheximide (CHX) for up to 4.5 h. Proteins were collected every 1.5 h. Western blotting against FLAG tag was performed. β-ACTIN detection was used as a control. hHOXA2 half-life was calculated based on hHOXA2 signal measurement with ImageJ. ($N > 3$) B: HEK293T cells were transfected with a combination of pExp plasmids coding for FLAG-hHOXA2, GST, GST-PPP1CB, GST-KPC2 and GST-KPC2 mutants (GST-KPC2ΔUBA_C-ter, GST-KPC2ΔUBA_N-ter and GST-KPC2ΔΔUBAs). hHOXA2 half-life was measured as in A. ($N = 3$).

treatment highlighted three additional phosphorylations (Fig. 9D).

Intriguingly however, CalA treatment did not have any impact on HOXA2 half-life (data not shown), supporting that PPP1CB enzymatic activity is not required for the PPP1CB effect on hHOXA2 stability. Inhibition of the phosphatase activity was also applied to evaluate its influence on hHOXA2 relocation, transcriptional activity and ubiquitination, without detectable impact. Being toxic to cells, CalA treatment was limited in time to remain compatible with cell survival. This restricted timing might be too short to allow highlighting the role of the enzymatic activity in PPP1CB-elicited effects. Together, although we

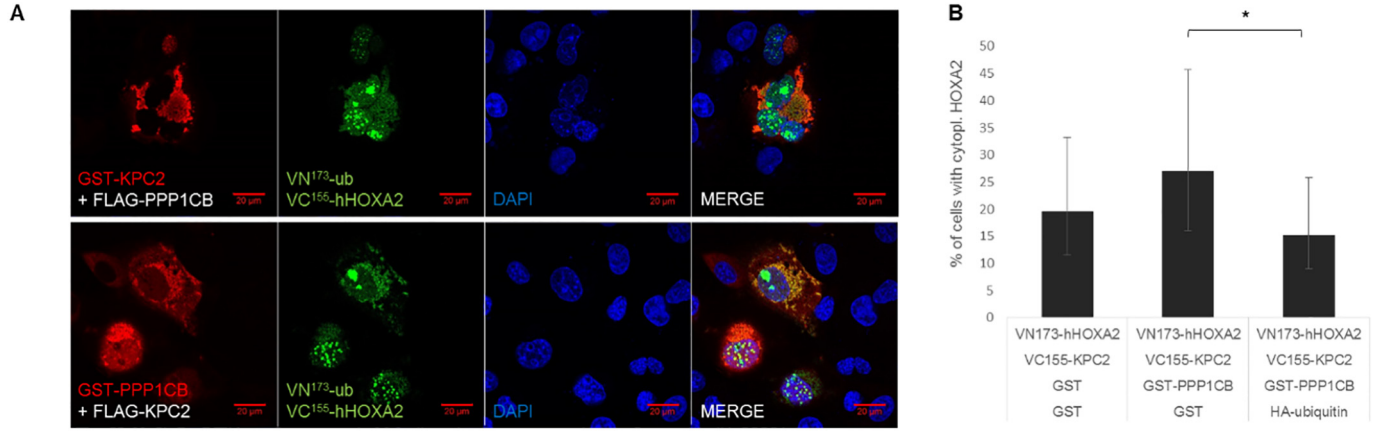

Fig. 8. PPP1CB and KPC2 co-localize with ubiquitin-hHOXA2 in the cytoplasm. A: COS7 cells were transfected with a combination of pExp plasmids coding for VN^{173}-ubiquitin, VC^{155}-hHOXA2, GST-KPC2, GST-PPP1CB, FLAG-PPP1CB and FLAG-KPC2. BiFC signal (green) shows ubiquitin-hHOXA2 interaction. Red signal was observed after immunofluorescence against GST. Nuclei were stained with DAPI (blue). Pictures were taken under confocal microscope. (N = 3) B: COS7 cells were transfected with a combination of pExp plasmids coding for VN^{173}-hHOXA2, VC^{155}-KPC2, GST, GST-PPP1CB and HA-ubiquitin-HA. Immunofluorescence detection of hHOXA2 was carried out in combination with BiFC. The percentage of cells presenting a predominant cytoplasmic hHOXA2 localization was calculated based on total transfected cells with ImageJ. Error bars = upper and lower intervals at 95%. *p-val $<$ 0.05. Scale bars = 20 µm. (N = 5, n = 3).

showed that hHOXA2 is phosphorylated by PP1, the involvement of the PPP1CB phosphatase activity on the regulation of HOXA2 activity requires further investigation.

4. Discussion

In the present study, we identified the protein phosphatase PPP1CB as a novel HOX interactor involved in regulating the activity of the HOXA2 protein. More specifically, we provided evidence that (1) PPP1CB interacts with hHOXA2 in the nucleus and the cytoplasm; (2) PPP1CB and hHOXA2 co-localize with KPC2, a hHOXA2 interactor previously described to regulate HOXA2 activity and cytoplasmic shuttling [23]; (3) both PPP1CB and KPC2 decrease hHOXA2 transcriptional activity directly and/or by interacting with PBX1A; (4) PPP1CB enhances the KPC2-dependent nucleocytoplasmic relocation of hHOXA2; (5) PPP1CB and KPC2 act to reduce the amount of ub-HOXA2 and to stabilize hHOXA2. Based on these observations, we propose an activity regulation model for hHOXA2 by which PPP1CB and KPC2 contribute to establish a “ready-to-use” cytoplasmic store of hHOXA2 protein (Fig. 10). In this model, KPC2 induces the nucleocytoplasmic shuttling of hHOXA2 and is assisted by PPP1CB, which either enhances this shuttling or assists in retaining hHOXA2 in the cytoplasm. In addition, hHOXA2 can be ubiquitinated and the interaction between ubiquitin and hHOXA2 forms is mostly located in the nucleus, presumably in association with chromatin. In the cytoplasm, ub-HOXA2 interaction co-localizes with KPC2 and PPP1CB, which both promote a decrease in ubiquitinated forms of hHOXA2. Finally, hHOXA2 interaction with KPC2 and PPP1CB, as well as its subcellular relocation and post-translational modifications, correlate with an increased hHOXA2 stability but a decreased hHOXA2 transcriptional activity. We therefore suggest that both PPP1CB and KPC2 regulate HOXA2 by implementing a cytoplasmic storage of inactive HOXA2 that upon a triggering signal may modify HOXA2 and send it back to the nucleus.

Based on our model, we propose that the decrease of hHOXA2 activity observed in the presence of PPP1CB and KPC2 could be correlated with the hHOXA2 relocation. However, our data suggest that PPP1CB could also decrease PREP1 and PBX1A activity. The co-localization between PBX1A, hHOXA2, KPC2 and PPP1CB in the cytoplasm, as well as their interaction, supports that the nucleo-cytoplasmic relocation of hHOXA2 could involve PBX1A, which in turn would also contribute to the activity regulation of hHOXA2 by KPC2 and PPP1CB. PBX1A is the best characterized HOX interactor and it has indeed been shown to bind an important subset of HOXA2 target enhancers in the embryo. PBX1A has therefore been hypothesized to critically contribute to HOXA2 target gene selection and/or activation in this context [43,44]. Both direct and indirect mechanisms could then take place in the hHOXA2 activity regulation by PPP1CB and KPC2.

In our model, PPP1CB is involved in the intra-cellular relocation of hHOXA2 induced by KPC2. Whether PPP1CB assists KPC2 in the nuclear exit of HOXA2 or contributes to the cytoplasmic retention of HOXA2 remains to be determined. For this, it will be interesting to assess the temporal order into which PPP1CB and KPC2 come into play to regulate HOXA2 relocation. Our data support that KPC2 and PPP1CB only interact with each other in the cytoplasm, suggesting that PPP1CB and KPC2 do not form a tripartite interaction with HOXA2 in the nucleus. Nevertheless, BiFC results indicate that PPP1CB can interact with HOXA2 in the nucleus. However, expression of PPP1CB alone, although showing interaction with hHOXA2 did not lead to hHOXA2 export. In contrast, KPC2 alone promoted hHOXA2 relocation, a phenomenon further enhanced by PPP1CB. These observations are in line with our previous study showing that KPC2-hHOXA2 binding stimulates hHOXA2 relocation and occurs before hHOXA2 nuclear export [23]. Therefore, we propose that PPP1CB is not involved in the direct export of hHOXA2 from the nucleus. It would rather be recruited by the KPC2-HOXA2 complex in the cytoplasm, where it could enhance the cytoplasmic retention of HOXA2.

For the first time, we highlighted here that hHOXA2 is ubiquitinated. Surprisingly, while KPC2 belongs to an E3 ubiquitin ligase, our results reveal that KPC2 and PPP1CB act in synergy to reduce the amount of ubiquitinated forms of hHOXA2, probably by recruiting a deubiquitinating enzyme. With the exception of p27, KPC2 interactions are poorly characterized [24,25]. Here, since deletion of the Ubiquitin Associated (UBA) domains of KPC2 reduced hHOXA2 deubiquitination, we suggest that KPC2 could be an anchor point for deubiquitinating enzyme recruitment. Lu et al. revealed that ubiquitin ligase and deubiquitinating enzyme could be part of the same complexes. Indeed, they showed that the deubiquitinating enzyme USP19 interacts with KPC1, the catalytic subunit of the KPC complex, and stabilizes KPC1 by deubiquitination [45]. In addition, since PPP1CB can compensate for the KPC2 loss of function when the UBA domains are deleted, this supports that PPP1CB would also present the capacity to recruit this or another deubiquitinating enzyme, even when KPC2 is devoid of its UBA domains.

While Bridoux et al. showed no difference in hHOXA2 stability when KPC2 is expressed [23], we reported here that KPC2, with or without expression of PPP1CB, increases hHOXA2 half-life. This

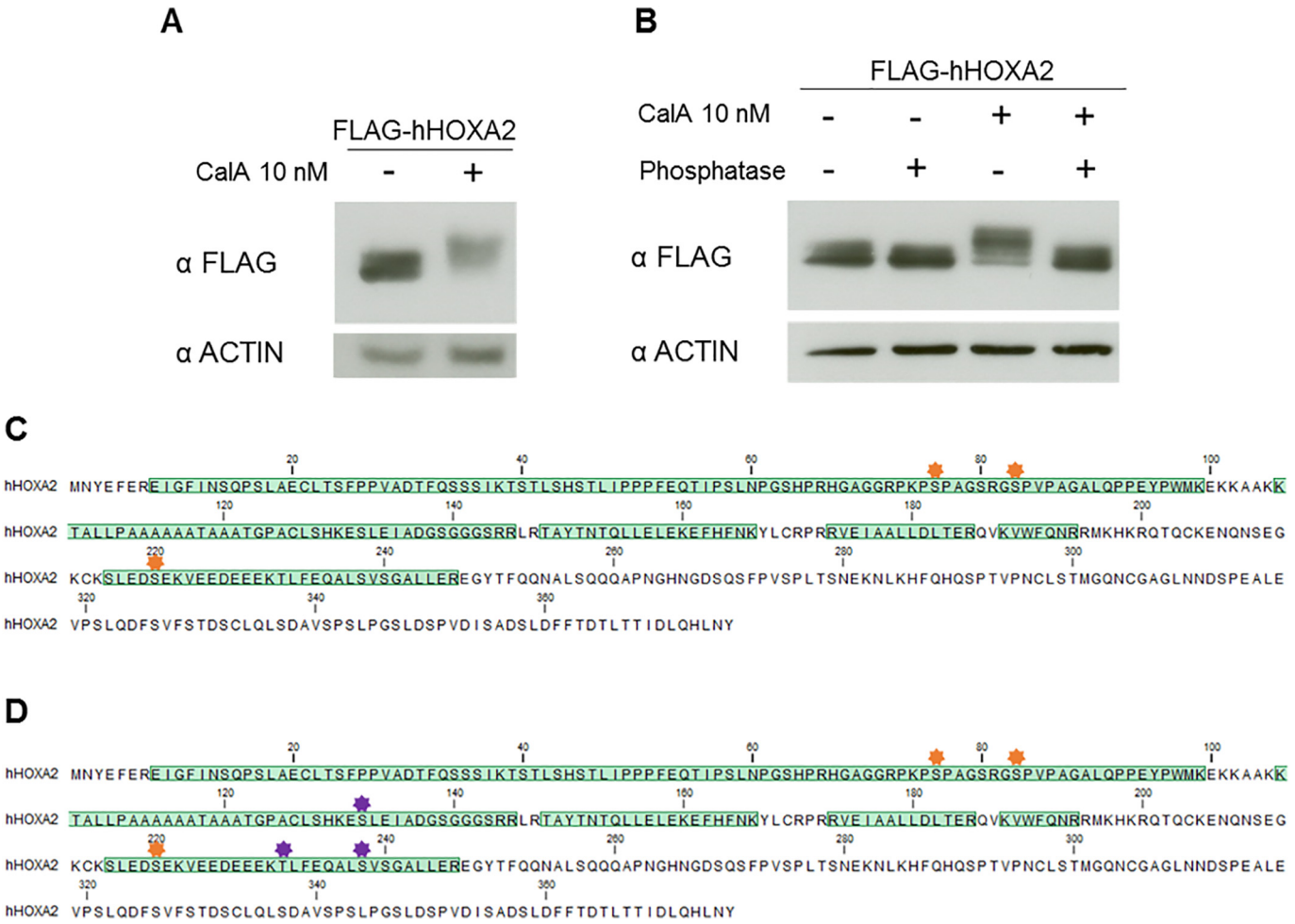

Fig. 9. PP1 phosphatase targets hHOXA2. A and B: HEK293T cells were transfected with a combination of pExp plasmids coding for FLAG-hHOXA2. To inhibit PP1 phosphatase activity, 48 h after transfection cells were treated 1 h with 10 nM Calyculin A (CalA). Western blotting against FLAG tag was performed to see the impact of CalA on hHOXA2 molecular weight (A). To validate the presence of phosphorylated forms of HOXA2, cell lysates treated or not with CalA were incubated 1 h30 with or without 20 U of Shrimp phosphatase (B). Disappearance of hHOXA2 molecular weight shift was observed by western blotting. β-ACTIN was detection used as a control. (N = 3) C and D: Mass spectrometry analysis of HOXA2. HEK293T cells were transfected with pExp plasmid coding for 6xHIS-hHOXA2. 32 h after transfection, cells were treated overnight with 6.6 μM MG132 to inhibit proteasomal degradation. 48 h after transfection, cells were treated 1 h with 6.6 μM MG132 combined with DMSO (**C**) or 5 nM CalA (D). Total protein extraction was passed through a Ni-NTA column to purify 6xHIS-hHOXA2 and analyzed by LC-MS/MS. Protein sequence covered by the MS analysis is shown in green. After DMSO treatment, three phosphorylations are found (C, orange marks) and, after CalA treatment, three new ones are appearing (D, purple marks).

suggests that the hHOXA2 deubiquitination induced by PPP1CB and KPC2 could be correlated with the longer hHOXA2 half-life. In fact, we showed that the KPC2 UBA domains are required to promote both the decrease in ub-hHOXA2 and the stabilization of hHOXA2. Surprisingly however, we observed that the loss of deubiquitination observed with KPC2 UBA mutants can be rescued by PPP1CB expression while the lack of hHOXA2 stabilization observed with the KPC2 mutants is not. That the impact of the UBA mutation on ub-hHOXA2 is rescued by PPP1CB but not its effect on hHOXA2 stabilization, reveals that hHOXA2 half-life cannot simply be correlated to its ubiquitination status. Since PPP1CB expression is sufficient to decrease ub-hHOXA2, it seems that PPP1CB has the capacity to bring KPC2, hHOXA2 and a deubiquitinating enzyme together, even in the absence of KPC2 UBA domains, but this is not sufficient to promote hHOXA2 stabilization.

We showed here that HOXA2 interacts with ubiquitin either at specific locations in the nucleus or in the cytoplasm where it co-localizes with PPP1CB and KPC2. Interestingly, we also found that ubiquitinated forms of HOXA2 are mainly present in the cellular fraction containing histone H3 and DNA. This suggests a scenario in which ub-hHOXA2 associates with the chromatin, while when the cell needs to reduce hHOXA2 activity, hHOXA2 is exported to the cytoplasm where PPP1CB and KPC2 act together to reduce HOXA2 ubiquitination.

In addition to ubiquitination, we also highlighted that hHOXA2 can be phosphorylated and is a PP1 target. Interestingly, PPP1CB was already shown to target and regulate proteins [31]. The histone deacetylase 7 (HDAC7) for example is dephosphorylated by the PPP1CB-MYPT1 complex in the cytoplasm [46]. HDAC7 dephosphorylation by PPP1CB-MYPT1 leads to a nuclear import of HDAC7, resulting in the repression of a pro-apoptotic orphan receptor. Based on this and other examples, one hypothesis would be that hHOXA2 dephosphorylation could affect hHOXA2 properties such as transcriptional activity. Nevertheless, Calyculin A treatment, a potent PP1 inhibitor, did not influence hHOXA2 stability in our experiments. The potential effect of PP1 phosphatase activity on hHOXA2 localization, transcriptional activity and ubiquitination state remain however to be investigated. In addition to HOXA2, PP1 phosphatase could also influence the activity of the KPC E3 ubiquitin ligase. Indeed, it is well-characterized that ubiquitin ligase activities are regulated by phosphorylation (reviewed in [47,48]). For instance, the CBL RING E3 ubiquitin ligase is activated by phosphorylation at Y371, which induces a conformational change abolishing its auto-inhibitory folding and which finally leads to E3 binding with E2 Ub-conjugating enzyme [49]. Besides CBL, other E3

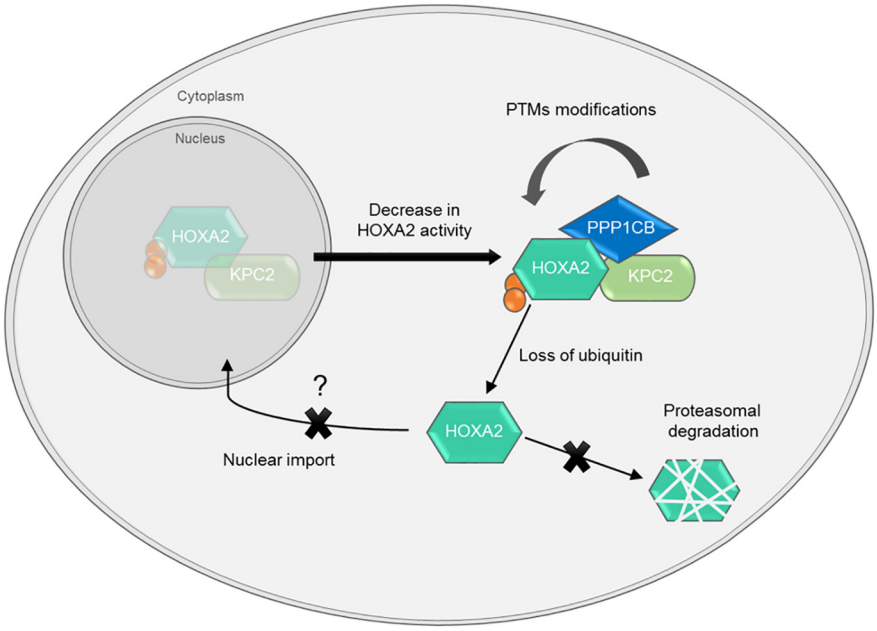

Fig. 10. Hypothetical model for HOXA2 activity regulation by PPP1CB and KPC2. See text for details.

ligases such as Parkin, APC/C or MDM2 are also subject to phosphorylations that regulate their activity (for reviews see [50–52]). The activity of PP1 towards KPC2 could explain why hHOXA2 needs to be in the cytoplasm to undergo post-translational regulation. Indeed, we could hypothesize that, once in the cytoplasm, HOXA2-KPC2 complex binds PPP1CB, which targets KPC2 or a KPC2-associated protein and therefore leads to HOXA2 regulation. However, further investigations are required to connect PP1 phosphatase activity and KPC ubiquitin ligase activity.

The nuclear PPP1CB-hHOXA2 interaction revealed by BiFC might underlie functional outcomes distinct from the activity regulation of hHOXA2 by intra-cellular shuttling. Indeed, it cannot be excluded that the interaction of PPP1CB affects multiple aspects of HOXA2 function. Most significantly, the PP1 phosphatase is a well-known histone modifier. PP1 targets the phosphorylated Ser10 and Ser28 residues of histone H3 and is known to act as a transcriptional co-regulator [53,54]. Among the 198 deregulated genes reported in DNA microarray analysis of nuclear PP1 inhibition in the mouse hippocampus, Gräff et al. revealed that *Trmp3* (Transient receptor potential cation channel, subfamily M, member 3) is downregulated when PP1 is inhibited [55]. Interestingly, this gene was also shown to be downregulated in the second branchial arches of *Hoxa2*-null mutant mice [56]. This observation calls for further investigation about the role of PP1 phosphatase as a HOXA2 transcriptional co-regulator at the chromatin.

That PPP1CB and KPC2 are active and contribute to HOX activities during embryogenesis requires functional validation which will be quite challenging considering the presumably pleiotropic activities of these enzymes. KPC2 functions during embryo development have not been addressed, but it has previously been shown that *Kpc2* is expressed conjointly with *Hoxa2* at different stages of embryogenesis [23]. Similarly, we showed here that *Ppp1cb* is expressed during mouse embryogenesis between E8.5 and E12.5, when *Hoxa2* is also expressed. In addition to PPP1CB involvement in muscle contraction [28], DNA repair [57] or heart modeling [58], a few studies reported that PPP1CB is also involved in early development. Jayashankar et al. highlighted that both zebrafish isoforms of PPP1CB (PPP1CBa and PPP1CBb), through their complex with MYPT1, are required for body axis elongation during gastrulation [59]. Double *Ppp1cba* and *Ppp1cbb* knock-down indeed present gastrulation defects such as a shortened and curved body axis, a reduction of yolk and posterior structures or a delay in epiboly. These phenotypes can be rescued by injection of *Ppp1cb* mRNA. In addition, Sun et al. showed in *Drosophila* that PPP1CB is involved in oocyte polarity through myosin dephosphorylation, and that a mutation inside the catalytic domain of PPP1CB is lethal [60]. Bridoux et al. and the present study show that KPC2 and PPP1CB have both the ability to interact with other hHOX proteins, namely HOXA1, HOXB1, HOXB2, HOXB5 and HOXD10 [23]. The activity regulation of HOX proteins by KPC2 and PPP1CB might therefore define a generic property shared by multiple if not all proteins of the HOX family.

5. Conclusion

In conclusion, this study presents a novel model for HOXA2 activity regulation, involving PPP1CB and KPC2. We suggest that these two regulators decrease HOXA2 transcriptional activity by inducing HOXA2 cytoplasmic relocation and post-translational modifications. As a consequence, PPP1CB and KPC2 would establish a ready-to-use cytoplasmic store of HOXA2 available for the cell when triggering HOXA2 activity is needed. This model could more generally apply to the full set of HOX proteins and opens new perspectives about how HOX proteins are modulated at the cellular level.

Transparency document

The Transparency document associated with this article can be found, in online version.

Credit author statement

René Rezsohazy: Resources, Funding acquisition, Conceptualization, Writing-Reviewing and Editing, Supervision. **Noémie Deneyer**: Conceptualization, Methodology, Investigation, Writing-Original draft preparation. **Laure Bridoux**: Conceptualization, Methodology, Investigation, Writing-Reviewing and Editing. **Céline Bombled**: Investigation. **Tamara Pringels**: Investigation. **Isabelle Bergiers**: Conceptualization, Methodology, Reviewing and Editing. **Sébastien Pyr dit Ruys**: Methodology, Reviewing and Editing. **Didier Vertommen**: Methodology, Reviewing and Editing. **Jean-Claude Twizere**: Conceptualization, Methodology.

Funding

ND is Research Fellow ('Aspirant') by the Belgian FRS-FNRS and L'Oréal-UNESCO "For women in science" laureate. JCT is Senior Research Associate ('Maitre de recherches') by the FRS-FNRS. This work was supported by the Crédits de Recherche CDR # 23607628 and CDR # 29112846 from the Belgian F.R.S. - FNRS, and the Fonds Spéciaux de Recherches from UCLouvain.

Acknowledgments

We are grateful to the IMABIOL platform from the UCLouvain for confocal microscopy support and especially Marie-Christine Eloy for her technical support. We thank the SMCS from the UCLouvain for its statistical advices, and more precisely Catherine Rasse for her statistical support. We acknowledge Philippe Bombaerts for laboratory technical help as well as Raphael Chiarelli for animal care.

Appendix A. Supplementary data

Supplementary data to this article can be found online at https://doi.org/10.1016/j.bbagrm.2019.07.005.

References

[1] T. Alexander, C. Nolte, R. Krumlauf, Hox genes and segmentation of the hindbrain and axial skeleton, Annu. Rev. Cell Dev. Biol. 25 (2009) 431–456.
[2] D. Frank, D. Sela-Donenfeld, Hindbrain induction and patterning during early vertebrate development, Cell. Mol. Life Sci. 76 (2019) 941–960.
[3] S.C. Quinonez, J.W. Innis, Human HOX gene disorders, Mol. Genet. Metab. 111 (2014) 4–15.
[4] S.W. Choo, S. Russell, Genomic approaches to understanding Hox gene function, Adv. Genet. 76 (2011) 55–91.
[5] R. Rezsohazy, A.J. Saurin, C. Maurel-Zaffran, Y. Graba, Cellular and molecular insights into Hox protein action, Development 142 (2015) 1212–1227.
[6] A.J. Saurin, M.C. Delfini, C. Maurel-Zaffran, Y. Graba, The generic facet of Hox protein function, Trends Genet. 34 (2018) 941–953.
[7] F. Lescroart, S. Zaffran, Hox and Tale transcription factors in heart development and disease, Int. J. Dev. Biol. 62 (2018) 837–846.
[8] S. Merabet, R.S. Mann, To be specific or not: the critical relationship between Hox and TALE proteins, Trends Genet. 32 (2016) 334–347.
[9] B. Gu, W.G. Zhu, Surf the post-translational modification network of p53 regulation, Int. J. Biol. Sci. 8 (2012) 672–684.
[10] T. Lu, G.R. Stark, NF-kappaB: regulation by methylation, Cancer Res. 75 (2015) 3692–3695.
[11] M. Won, H.S. Byun, K.A. Park, G.M. Hur, Post-translational control of NF-kappaB signaling by ubiquitination, Arch. Pharm. Res. 39 (2016) 1075–1084.
[13] A. Draime, L. Bridoux, Y. Graba, R. Rezsohazy, Post-translational modifications of HOX proteins, an underestimated issue, Int. J. Dev. Biol. 62 (2018) 733–744.
[14] M. Primon, K.D. Hunter, H.S. Pandha, R. Morgan, Kinase regulation of HOX transcription factors, Cancers (Basel) 11 (2019) E508.
[15] E.A. Eklund, A. Jalava, R. Kakar, Tyrosine phosphorylation of HoxA10 decreases DNA binding and transcriptional repression during interferon gamma -induced differentiation of myeloid leukemia cell lines, J. Biol. Chem. 275 (2000) 20117–20126.
[16] E.A. Eklund, I. Goldenberg, Y. Lu, J. Andrejic, R. Kakar, SHP1 protein-tyrosine phosphatase regulates HoxA10 DNA binding and transcriptional repression activity in undifferentiated myeloid cells, J. Biol. Chem. 277 (2002) 36878–36888.
[17] R. Jiang, L. Ding, J. Zhou, C. Huang, Q. Zhang, Y. Jiang, J. Liu, Q. Yan, X. Zhen, J. Sun, G. Yan, H. Sun, Enhanced HOXA10 sumoylation inhibits embryo implantation in women with recurrent implantation failure, Cell. Death Discov. 3 (2017) 17057.
[18] L.H. Zhu, L.H. Sun, Y.L. Hu, Y. Jiang, H.Y. Liu, X.Y. Shen, X.Y. Jin, X. Zhen, H.X. Sun, G.J. Yan, PCAF impairs endometrial receptivity and embryo implantation by down-regulating beta3-integrin expression via HOXA10 acetylation, J. Clin. Endocrinol. Metab. 98 (2013) 4417–4428.
[19] X. Li, C. Murre, W. McGinnis, Activity regulation of a Hox protein and a role for the homeodomain in inhibiting transcriptional activation, EMBO J. 18 (1999) 198–211.
[20] I. Bergiers, L. Bridoux, N. Nguyen, J.C. Twizere, R. Rezsohazy, The homeodomain transcription factor Hoxa2 interacts with and promotes the proteasomal degradation of the E3 ubiquitin protein ligase RCHY1, PLoS One 8 (2013) e80387.
[21] P. Lamesch, N. Li, S. Milstein, C. Fan, T. Hao, G. Szabo, Z. Hu, K. Venkatesan, G. Bethel, P. Martin, J. Rogers, S. Lawlor, S. McLaren, A. Dricot, H. Borick, M.E. Cusick, J. Vandenhaute, I. Dunham, D.E. Hill, M. Vidal, hORFeome v3.1: a resource of human open reading frames representing over 10,000 human genes, Genomics 89 (2007) 307–315.
[22] L. Bridoux, N. Deneyer, I. Bergiers, R. Rezsohazy, Molecular analysis of the HOXA2-dependent degradation of RCHY1, PLoS One 10 (2015) e0141347.
[23] L. Bridoux, I. Bergiers, A. Draime, M. Halbout, N. Deneyer, J.C. Twizere, R. Rezsohazy, KPC2 relocalizes HOXA2 to the cytoplasm and decreases its transcriptional activity, Biochim. Biophys. Acta 1849 (2015) 1298–1311.
[24] T. Hara, T. Kamura, S. Kotoshiba, H. Takahashi, K. Fujiwara, I. Onoyama, M. Shirakawa, N. Mizushima, K.I. Nakayama, Role of the UBL-UBA protein KPC2 in degradation of p27 at G1 phase of the cell cycle, Mol. Cell. Biol. 25 (2005) 9292–9303.
[25] S. Kotoshiba, T. Kamura, T. Hara, N. Ishida, K.I. Nakayama, Molecular dissection of the interaction between p27 and Kip1 ubiquitylation-promoting complex, the ubiquitin ligase that regulates proteolysis of p27 in G1 phase, J. Biol. Chem. 280 (2005) 17694–17700.
[26] P. Cohen, Protein phosphatase 1 - targeted in many directions, J. Cell Sci. 115 (2002) 241–256.
[27] L. Korrodi-Gregorio, S.L. Esteves, M. Fardilha, Protein phosphatase 1 catalytic isoforms: specificity toward interacting proteins, Transl. Res. 164 (2014) 366–391.
[28] D.R. Alessi, L.K. Macdougall, M.M. Sola, M. Ikebe, P. Cohen, The control of protein phosphatase-1 by targetting subunits. The major myosin phosphatase in avian smooth muscle is a novel form of protein phosphatase-1, Eur. J. Biochem. 210 (1992) 1023–1035.
[29] M.E. Grassie, L.D. Moffat, M.P. Walsh, J.A. MacDonald, The myosin phosphatase targeting protein (MYPT) family: a regulated mechanism for achieving substrate specificity of the catalytic subunit of protein phosphatase type 1delta, Arch. Biochem. Biophys. 510 (2011) 147–159.
[30] E. Scotto-Lavino, M. Garcia-Diaz, G. Du, M.A. Frohman, Basis for the isoform-specific interaction of myosin phosphatase subunits protein phosphatase 1c beta and myosin phosphatase targeting subunit 1, J. Biol. Chem. 285 (2010) 6419–6424.
[31] T. Ryan, M. Shelton, J.P. Lambert, B. Malecova, S. Boisvenue, M. Ruel, D. Figeys, P.L. Puri, I.S. Skerjanc, Myosin phosphatase modulates the cardiac cell fate by regulating the subcellular localization of Nkx2.5 in a Wnt/rho-associated protein kinase-dependent pathway, Circ. Res. 112 (2013) 257–266.
[32] G. Goudet, S. Delhalle, F. Biemar, J.A. Martial, B. Peers, Functional and cooperative interactions between the homeodomain PDX1, Pbx, and Prep1 factors on the somatostatin promoter, J. Biol. Chem. 274 (1999) 4067–4073.
[33] S. Remacle, C. Shaw-Jackson, C. Matis, X. Lampe, J. Picard, R. Rezsohazy, Changing homeodomain residues 2 and 3 of Hoxa1 alters its activity in a cell-type and enhancer dependent manner, Nucleic Acids Res. 30 (2002) 2663–2668.
[34] C. Matis, P. Chomez, J. Picard, R. Rezsohazy, Differential and opposed transcriptional effects of protein fusions containing the VP16 activation domain, FEBS Lett. 499 (2001) 92–96.
[35] X. Lampe, O.A. Samad, A. Guiguen, C. Matis, S. Remacle, J.J. Picard, F.M. Rijli, R. Rezsohazy, An ultraconserved Hox-Pbx responsive element resides in the coding sequence of Hoxa2 and is active in rhombomere 4, Nucleic Acids Res. 36 (2008) 3214–3225.
[36] J.F. Rual, K. Venkatesan, T. Hao, T. Hirozane-Kishikawa, A. Dricot, N. Li, G.F. Berriz, F.D. Gibbons, M. Dreze, N. Ayivi-Guedehoussou, N. Klitgord, C. Simon, M. Boxem, S. Milstein, J. Rosenberg, D.S. Goldberg, L.V. Zhang, S.L. Wong, G. Franklin, S. Li, J.S. Albala, J. Lim, C. Fraughton, E. Llamosas, S. Cevik, C. Bex, P. Lamesch, R.S. Sikorski, J. Vandenhaute, H.Y. Zoghbi, A. Smolyar, S. Bosak, R. Sequerra, L. Doucette-Stamm, M.E. Cusick, D.E. Hill, F.P. Roth, M. Vidal, Towards a proteome-scale map of the human protein-protein interaction network, Nature 437 (2005) 1173–1178.
[37] B. Lambert, J. Vandeputte, S. Remacle, I. Bergiers, N. Simonis, J.C. Twizere, M. Vidal, R. Rezsohazy, Protein interactions of the transcription factor Hoxa1, BMC Dev. Biol. 12 (2012) 29.
[38] B. Hutlet, N. Theys, C. Coste, M.-T. Ahn, K. Doshishti-Agolli, B. Lizen, F. Gofflot, Systematic expression analysis of Hox genes at adulthood reveals novel patterns in the central nervous system, Brain Struct. Funct. 221 (2016) 1223–1243.
[39] F.M. Rijli, M. Mark, S. Lakkaraju, A. Dierich, P. Dollé, P. Chambon, A homeotic transformation is generated in the rostral branchial region of the head by disruption of *Hoxa-2*, which acts as a selector gene, Cell 75 (1993) 1333–1349.
[40] M. Gendron-Maguire, M. Mallo, M. Zhang, T. Gridley, Hoxa-2 mutant mice exhibit homeotic transformation of skeletal elements derived from cranial neural crest, Cell 75 (1993) 1317–1331.
[41] C. Cid, L. Garcia-Bonilla, E. Camafeita, J. Burda, M. Salinas, A. Alcazar, Proteomic characterization of protein phosphatase 1 complexes in ischemia-reperfusion and ischemic tolerance, Proteomics 7 (2007) 3207–3218.
[42] M. Akutsu, I. Dikic, A. Bremm, Ubiquitin chain diversity at a glance, J. Cell Sci. 129 (2016) 875–880.
[43] E. Longobardi, D. Penkov, D. Mateos, G. De Florian, M. Torres, F. Blasi, Biochemistry of the tale transcription factors PREP, MEIS, and PBX in vertebrates, Dev. Dyn. 243 (2014) 59–75.
[44] S. Amin, I.J. Donaldson, D.A. Zannino, J. Hensman, M. Rattray, M. Losa, F. Spitz, F. Ladam, C. Sagerstrom, N. Bobola, Hoxa2 selectively enhances Meis binding to change a branchial arch ground state, Dev. Cell 32 (2015) 265–277.
[45] Y. Lu, O.A. Adegoke, A. Nepveu, K.I. Nakayama, N. Bedard, D. Cheng, J. Peng, S.S. Wing, USP19 deubiquitinating enzyme supports cell proliferation by stabilizing KPC1, a ubiquitin ligase for p27Kip1, Mol. Cell. Biol. 29 (2009) 547–558.
[46] M. Parra, T. Mahmoudi, E. Verdin, Myosin phosphatase dephosphorylates HDAC7, controls its nucleocytoplasmic shuttling, and inhibits apoptosis in thymocytes, Genes Dev. 21 (2007) 638–643.
[47] P. Filipcik, J.R. Curry, P.D. Mace, When worlds collide-mechanisms at the Interface between phosphorylation and ubiquitination, J. Mol. Biol. 429 (2017) 1097–1113.
[48] N. Zheng, N. Shabek, Ubiquitin ligases: structure, function, and regulation, Annu. Rev. Biochem. 86 (2017) 129–157.
[49] H. Dou, L. Buetow, A. Hock, G.J. Sibbet, K.H. Vousden, D.T. Huang, Structural basis for autoinhibition and phosphorylation-dependent activation of c-Cbl, Nat. Struct.

Mol. Biol. 19 (2012) 184–192.
[50] N. Panicker, V.L. Dawson, T.M. Dawson, Activation mechanisms of the E3 ubiquitin ligase parkin, Biochem. J. 474 (2017) 3075–3086.
[51] D.W. Meek, T.R. Hupp, The regulation of MDM2 by multisite phosphorylation–opportunities for molecular-based intervention to target tumours? Semin. Cancer Biol. 20 (2010) 19–28.
[52] H. Yamano, APC/C: current understanding and future perspectives [version 1; peer review: 3 approved], F1000Res, 8 (2019) 725.
[53] J.-Y. Hsu, Z.-W. Sun, X. Li, M. Reuben, K. Tatchell, D.K. Bishop, J.M. Grushcow, C.J. Brame, J.A. Caldwell, D.F. Hunt, R. Lin, M.M. Smith, C.D. Allis, Mitotic phosphorylation of histone H3 is governed by Ipl1/aurora kinase and Glc7/PP1 phosphatase in budding yeast and nematodes, Cell 102 (2000) 279–291.
[54] H. Goto, Y. Yasui, E.A. Nigg, M. Inagaki, Aurora-B phosphorylates histone H3 at serine28 with regard to the mitotic chromosome condensation, Genes Cells 7 (2002) 11–17.
[55] J. Graff, K. Koshibu, A. Jouvenceau, P. Dutar, I.M. Mansuy, Protein phosphatase 1-dependent transcriptional programs for long-term memory and plasticity, Learn. Mem. 17 (2010) 355–363.
[56] I.J. Donaldson, S. Amin, J.J. Hensman, E. Kutejova, M. Rattray, N. Lawrence, A. Hayes, C.M. Ward, N. Bobola, Genome-wide occupancy links Hoxa2 to Wnt-beta-catenin signaling in mouse embryonic development, Nucleic Acids Res. 40 (2012) 3990–4001.
[57] C.Y. Lin, B.C. Tan, H. Liu, C.J. Shih, K.Y. Chien, C.L. Lin, B.Y. Yung, Dephosphorylation of nucleophosmin by PP1beta facilitates pRB binding and consequent E2F1-dependent DNA repair, Mol. Biol. Cell 21 (2010) 4409–4417.
[58] R. Liu, R.N. Correll, J. Davis, R.J. Vagnozzi, A.J. York, M.A. Sargent, A.C. Nairn, J.D. Molkentin, Cardiac-specific deletion of protein phosphatase 1beta promotes increased myofilament protein phosphorylation and contractile alterations, J. Mol. Cell. Cardiol. 87 (2015) 204–213.
[59] V. Jayashankar, M.J. Nguyen, B.W. Carr, D.C. Zheng, J.B. Rosales, J.B. Rosales, D.C. Weiser, Protein phosphatase 1 beta paralogs encode the zebrafish myosin phosphatase catalytic subunit, PLoS One 8 (2013) e75766.
[60] Y. Sun, Y. Yan, N. Denef, T. Schupbach, Regulation of somatic myosin activity by protein phosphatase 1beta controls Drosophila oocyte polarization, Development 138 (2011) 1991–2001.